UBEST

Understanding the biogeochemical buffering capacity of estuaries relative to climate change and anthropogenic inputs

Report 8

Calibration and validation of the 3D hydrodynamic model of the Ria Formosa

Partners

LNEC LABORATÓRIO NACIONAL DE ENGENHARIA CIVIL

Funding

PTDC/AAG-MAA/6899/2014

Authors:

Alexandra Rosa[1], José Jacob[1], Marta Rodrigues[2], André Fortunato[2], Alexandra Cravo[1]

[1]**Universidade do Algarve**

[2]**Laboratório Nacional de Engenharia Civil**

October, 2019

Abstract

The project UBEST aims to improve the global understanding of the biogeochemical buffering capacity of the Ria Formosa coastal lagoon (south of Portugal), one of the study areas, and its susceptibility to future scenarios of anthropogenic inputs and climate change. A better understanding of the processes that affect the productivity of the Ria Formosa is essential for its preservation and sustainable management. To achieve the main goal of UBEST, the hydrodynamic model SCHISM was implemented in this coastal lagoon, as described in this report. The model was calibrated and validated with *in situ* data acquired in previous seasonal campaigns performed in the Ria Formosa, and also with contemporary data acquired by the Real-Time Observatory station installed since May 2017. *In situ* measurements of temperature and salinity using multiparametric probes and sea surface elevation records from four pressure transducers installed in different locations in the lagoon were used to validate the hydrodynamic model in different seasons. The results revealed a good performance of the model in the representation of the hydrodynamic circulation within the lagoon and the spatial and temporal variations of the temperature and salinity, except some limitations at the edges of this coastal lagoon. The implementation of the hydrodynamic model and a further coupling of a biogeochemical model will contribute to simulate futures scenarios of climatic changes and anthropogenic inputs.

Keywords: Numerical modelling, hydrodynamic model, Ria Formosa

Table of Contents

Table of Figures

Table of Tables

1. Introduction

The project UBEST, funded by the Fundação para a Ciência e Tecnologia (PTDC/AAG-MAA/6899/2014), aims to improve the global understanding of the biogeochemical buffering capacity of estuaries and its susceptibility relative to future scenarios of anthropogenic inputs and climate change. In this context, models are particularly important to predict the consequences of future global changes. In order to be reliable, models must be implemented, tested, calibrated and validated, a task that is led by the LNEC partner in this project. A multidisciplinary approach was undertaken, assembling high-resolution numerical modelling with *in situ* data from field campaigns. The Ria Formosa is one of the case studies and, as a coastal lagoon located at the land-ocean boundary, is particularly vulnerable to the pressures mentioned before, since these can influence the water quality (e.g. availability of nutrients, chlorophyll-a and dissolved oxygen), ecosystem dynamics (e.g. buffering capacity) and consequently affect its services. The implementation of the hydrodynamic model for the Ria Formosa was performed by the first author under the supervision of the LNEC team members, while the field campaigns in this system were performed by the team of the University of Algarve.

This report describes the implementation of the three-dimensional hydrodynamic numerical model SCHISM (Semi-implicit Cross-scale Hydroscience Integrated System Model) in the Ria Formosa. This hydrodynamic model was developed based on previous applications (e.g. Fabião *et al.*, 2016) implemented by the LNEC team. Significant improvements and updates in the grid, bathymetry parameterization, model version and boundary conditions were introduced herein. The results demonstrate the performance of the model in reproducing the main circulation patterns within the lagoon, as well as the salinity and temperature of the water.

The report is organized in five chapters, apart from this Introduction chapter. The study area is described in Chapter 2, while the SCHISM model in Chapter 3. The implementation of the barotropic and of the baroclinic models are presented in Chapters 4 and 5, respectively. To finish, the Chapter 6 presents the conclusions.

2. Study area

The Ria Formosa is a highly productive coastal lagoon located in the south coast of Portugal, where several human activities take part (Newton *et al*., 2014). This system is recognized as a Natural Park since 1987 and internationally as a Ramsar site, being part of the Natura 2000 Network (Newton and Mudge, 2003). It includes a barrier island system and extends along 55 km (west-east) and 6 km of width (north-south), with a triangular shape. The mean depth is 3.5 m, ranging from 6 to 13 m in the main channels (Falcão and Vale, 1990; Barbosa, 2010; Cravo *et al*., 2014). The Ria Formosa is delimited on its seaward side by 5 sandy barrier islands (Deserta, Culatra, Armona, Tavira and Cabanas), 2 peninsulas (Ancão and Cacela) (Ferreira *et al*., 2003) and 6 inlets. The lagoon can be divided into three sectors (eastern, central and western), which are separated by the Tavira and the Armona inlets, respectively. These sectors are interconnected by a network of channels, which allows the recirculation of water within the lagoon and promote the exchange with the Atlantic Ocean through the inlets. The western sector is responsible for 90% of the water exchanged with the ocean (Pacheco *et al*., 2010). Within the scope of Water Framework Directive (WFD), the Ria Formosa encompasses five water bodies (Figure 2.1), associated to the water circulation patterns and human pressures (Ferreira *et al*., 2005, 2006).

Figure 2.1 – Location of the water bodies (WB) delimited by different colors, of the sampling stations (green circles), of the Real-Time Observatory (RTO) and of the deployed pressure transducers (orange stars).

The Ria Formosa is influenced by semidiurnal tides with a mean tidal range of *ca.* 2 m, ranging from 1.5 m to 3.5 m (Jacob and Cravo, 2019). Tides are the main driver of the water renewal in the

lagoon, responsible for 50% to 75% of daily water renewal (Newton and Mudge, 2003; Tett *et al*., 2003; Mudge *et al*., 2008). The wind has a small influence on water circulation and mass transport in this coastal lagoon, due to a moderate average wind speed (Salles *et al*., 2005; Fabião *et al*., 2016; Jacob and Cravo, 2019). Due to its low mean depth, strong tidal currents, high rate of water exchange and low freshwater inputs, this coastal lagoon can be considered vertically well mixed, without evidence of saline and/or thermal stratification. However, during periods of heavy rainfall, the influence of freshwater can be evident, particularly in Tavira, where the only permanent source of freshwater is located (Gilão River) (Newton and Mudge, 2003). Regarding past studies coupling data acquisition and numerical modelling, few studies have been developed and those are focused on the hydrodynamics characteristics of the western sector of the lagoon (Salles, 2001; Martins *et al*., 2003; Salles *et al*., 2005; Dias *et al*., 2009; Jacob *et al*., 2012 and 2013), whereas studies considering the global system of the Ria Formosa are scarce (Pacheco *et al*., 2010; Fabião *et al*., 2016; Malta *et al*., 2017).

3. Description of the SCHISM model

The hydrodynamic simulations were performed using the SCHISM 3D numerical model (Semi-implicit Cross-scale Hydroscience Integrated System Model) (Zhang *et al*., 2016), an open-source community-supported modeling system designed for simulation of 3D baroclinic circulation. The model is a derivative product built from the original SELFE model (Zhang and Baptista 2008), with many enhancements and upgrades, including new extension to large-scale eddying regime and a seamless cross-scale capability from creek to ocean (Zhang *et al*., 2016). SCHISM solves the three-dimensional shallow waters equations and calculates the free-surface elevation and the 3D water velocity, salinity and temperature fields using finite-element and finite-volume schemes. The continuity and momentum equations are solved simultaneously, thus bypassing the most severe stability restrictions (e.g. associated with the Courant number).

In SCHISM, mass conservation can be enforced by upwind or finite-volume transport algorithm (TVD^2) methods. It also naturally incorporates wetting and drying suitable for inundation studies. It uses a highly efficient semi-implicit finite-element Eulerian-Lagrangian algorithm to solve the Navier-Stokes equations (in either hydrostatic or non-hydrostatic form), to address a wide range of physical processes. The 3D domain is discretized by an unstructured mixed triangular/quadrangular grid in the horizontal and by hybrid SZ coordinates or LSC^2 (Zhang *et al*., 2015) along the vertical, which allows a greater flexibility in representing the bathymetry. The model is fully parallelized, allowing to optimize the computing times in high-resolution and year-long simulations, in particular by taking advantage of the computational resources belonging to the FCT's National Distributed Computing Infrastructures, the LNEC's cluster. The hydrodynamic model is fully coupled to a biogeochemical model (Rodrigues *et al*., 2009; Rodrigues *et al*., 2012), which simulates the cycles of carbon, nitrogen, phosphorus and silica for the lower trophic levels.

The SCHISM system has been extensively tested against standard ocean/coastal benchmarks and applied to a number of regional seas/bays/estuaries around the world in the context of general circulation, tsunami and storm-surge inundation, water quality, oil spill, sediment transport, coastal ecology, and wave-current interaction (e.g. Rodrigues and Fortunato, 2017; Chiu *et al*., 2018; Li *et al*., 2018; Linares *et al*., 2019). A detailed description of the model can be found in Zhang *et al*. (2016).

4. Implementation of the barotropic model

4.1 Data for the model calibration and validation

The hydrodynamic model was first calibrated in 3D barotropic mode. This application was based on the previous application of SELFE 3D (Zhang and Baptista, 2008) in the Ria Formosa by Fabião *et al*. (2016). The model calibration was performed by comparison of the model results with the sea surface elevation data measured by the Instituto Hidrográfico (Instituto Hidrográfico, 1981) between October 1979 and October 1980 at 11 stations located along the Ria Formosa and in the adjacent coastal area (Figure 4.1). The model was then validated by comparing the model results with sea surface elevation and current velocity data sets from the field campaigns carried out in the western sector of the Ria Formosa between October and December 2011 within the scope of project COALA (Jacob *et al*., 2012; Fabião *et al*., 2016). The current velocities were acquired hourly along a cross-section at the Faro-Olhão and Armona inlets and at the Faro and Olhão channels. The mean velocity component perpendicular to the cross-section was determined as the ratio between the volumetric flow (or discharge) through the cross-section and its area. The sea surface elevation was measured for a period of 2 months (since 14 October 2011 to 14 December 2011), with a sampling interval of 10 min, at the Deserta Island Pier (DIP) and the Faro Commercial Port (FCP) (Figure 4.2).

Figure 4.1 – Horizontal grid and bathymetry (1980s, MSL – mean sea level). Location of the sampling stations.

Figure 4.2 – Horizontal grid and bathymetry (2011, MSL – mean sea level). Location of the sampling stations.

4.2 Model calibration

4.2.1 Model setup

For the calibration, the domain was discretized in a horizontal grid with 90096 nodes and 177073 elements and a spatial resolution varying from 10 m to 6 km (Figure 4.1), and in a vertical domain with SZ levels (7 S levels in the upper 100 m and 4 Z levels between 100 m and 775 m). Bathymetric information from 1980 was used in the domain (Figure 4.1). The model was forced only by tides at the oceanic boundary. 14 tidal constituents were imposed (Z0, MSf, Q1, O1, P1, K1, N2, M2, S2, K2, MN4, M4, MS4 e M6). The time step was set to 30 s, as numerical oscillations were observed with a lower time step (15 s). During the calibration several simulations were performed, by changing different parameters, namely the bottom friction, the oceanic boundary forcing and the grid resolution at the oceanic boundary. Three tests were performed to optimize the bottom roughness: constant drag coefficient; depth-dependent drag coefficient, estimated based on Dias and Lopes (2006); and variable drag coefficient, according to the land use based on the CORINE Land Cover 2006. Regarding to the tidal forcing, two regional models were tested: Fortunato *et al*. (2002) and Fortunato *et al*. (2016).

4.2.2 Results

Data and model results were both harmonically analyzed and then synthesized for eight tidal constituents (MSF, O1, K1, M2, S2, M4, MS4, M6). The Root Mean Square Error (RMSE; standard deviation of the residuals) between data and model results was computed and compared with previous applications in the Ria Formosa (Dias *et al.*, 2009; Bruneau *et al.*, 2010; Fabião *et al.*, 2016; Figure 4.3). The best results were obtained using the horizontally varying drag coefficient based on the land use and the regional model of Fortunato *et al.* (2016) to force the oceanic boundary. The results are thus presented for this simulation. The RMSE ranged between 3 and 13 cm, showing a good agreement between the SCHISM model and the field data. The RMSE values were significantly lower than those presented by Dias *et al.* (2009), that ranged from 7 to 21 cm, and are of the same order of magnitude than those presented by the others authors. The differences may result from differences in the horizontal grid (in particular, the grid used in the present application has a higher resolution than the one used by Dias *et al.* (2009)) and also from the model itself, since the models used in these applications are different.

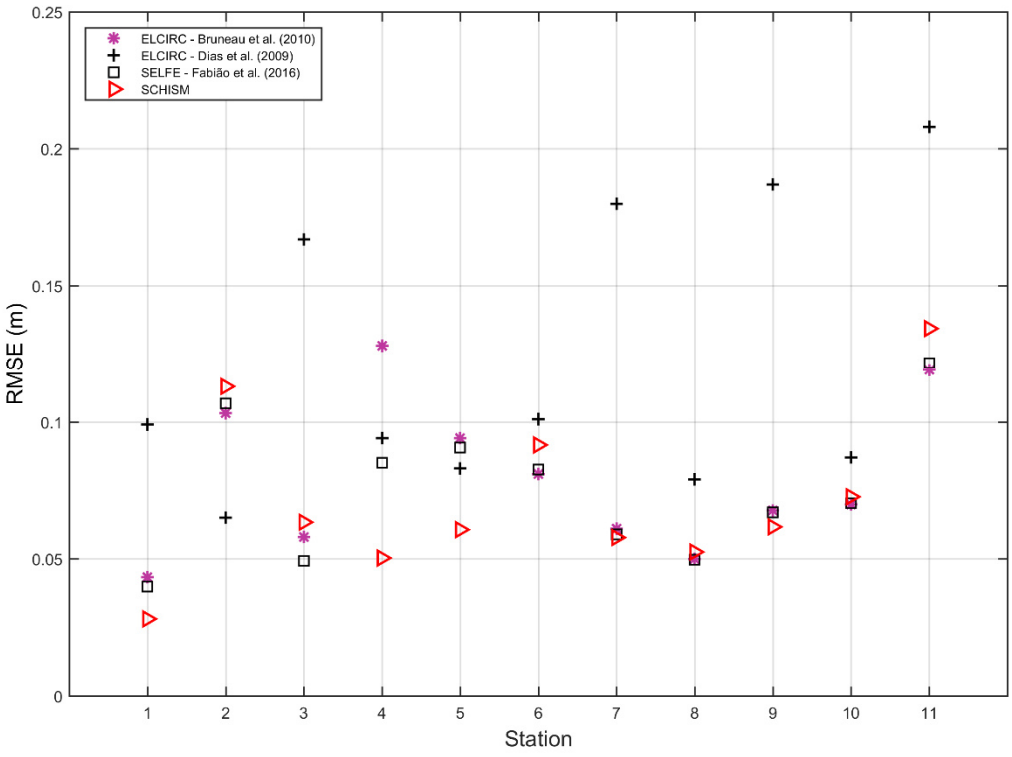

Figure 4.3 – Comparison of the Root Mean Square Error (m) for sea surface elevation between previous applications (ELCIRC – Bruneau *et al.* (2010), ELCIRC – Dias *et al.* (2009), SELFE – Fabião *et al.* (2016)) and the best result obtained from SCHISM model simulations for each station.

4.3 Model validation

4.3.1 Model setup

Within the scope of project COALA several campaigns were performed in the Ancão, Faro-Olhão and Armona inlets and in the Faro and Olhão channels, between October and December 2011. To validate the model, sea surface elevation and current velocities simulated by the SCHISM 3D model were compared with the field data described in section 4.1. The bathymetry was updated with the most recent data available, as described by Bruneau *et al.* (2010) – Figure 4.2. This simulation was based on the setup described in section 4.2 for SCHISM model. It was performed for 62 days, starting on 10/10/2011.

4.3.2 Results

The comparison of the sea surface elevation series for the Deserta Island Pier and the Faro Commercial Port are presented in the Figure 4.4 and Figure 4.5 and the RMSE between the field data and the simulations from SELFE (2D and 3D) and SCHISM 3D are presented in Table 4.1.

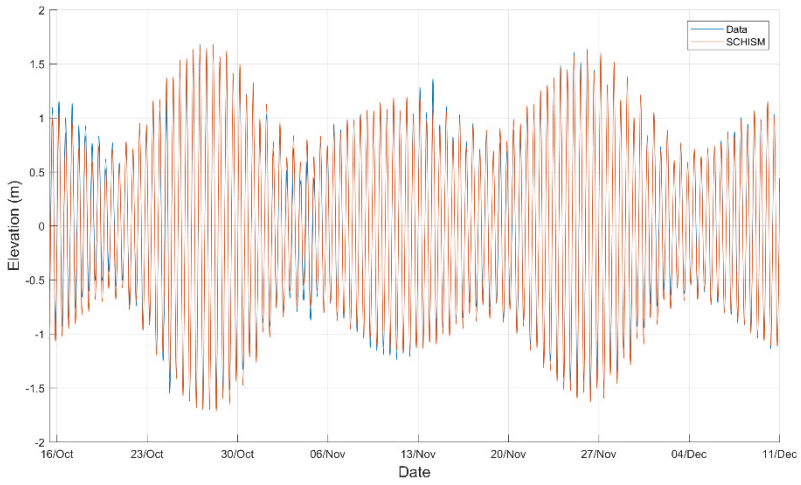

Figure 4.4 – Comparison of the sea surface elevation acquired in the Deserta Island Pier (DIP) with the SCHISM simulation.

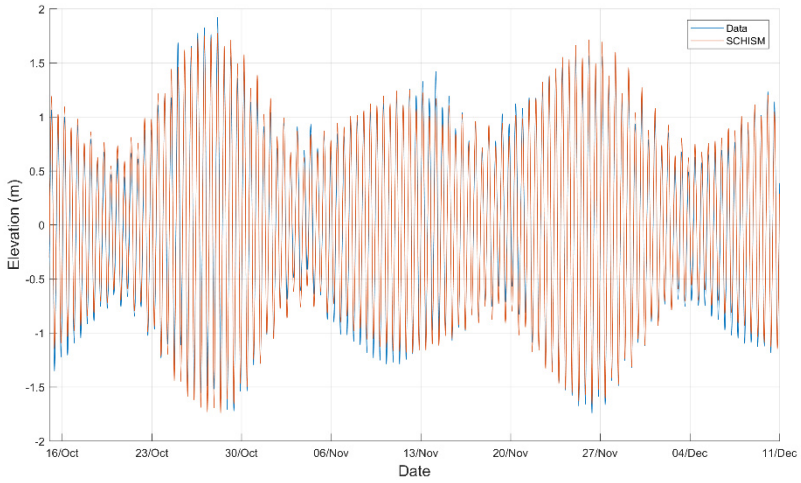

Figure 4.5 – Comparison of the sea surface elevation acquired in the Faro Commercial Pier (FCP) with the SCHISM simulation.

Table 4.1 – Root Mean Square Error (cm) between the sea surface elevation recorded at Deserta Island Pier (DIP) and Faro Commercial Port (FCP) stations and the simulations performed by SELFE 2D, SELFE 3D (Fabião *et al.*, 2016) and SCHISM 3D models.

Model	RMSE (cm)	
	DIP	FCP
SELFE 2D (COALA)	8.0	12.1
SELFE 3D (Fabião *et al.*, 2016)	8.7	10.9
SCHISM 3D	8.2	11.5

The RMSE for the Deserta Island Pier and the Faro Commercial Port are *ca.* 8 cm and 11 cm, respectively. Comparing the RMSE between the 3D models, SCHISM showed lower errors in the Deserta Island Pier, but slightly higher in the Faro Commercial Port. Nevertheless, in both cases the errors are within a range considered acceptable in the literature.

The comparison between the average current velocities measured in the cross-section at Faro-Olhão and Armona inlets and at Faro and Olhão channels and simulated by SELFE 3D (Fabião *et al.*, 2016) and SCHISM 3D applications in the Ria Formosa are presented in Figure 4.6 to Figure 4.9, for both spring tide and neap tide conditions. Results show a very good agreement between the model and the current velocities acquired during the field campaigns. Both models tend to underestimate the mean velocities at Faro-Olhão inlet and Faro channel and to overestimate them at the Armona inlet and the Olhão channel, particularly in spring tides. These differences can be associated with some uncertainty in the bathymetric data, since in some areas of the domain the bathymetry is not contemporaneous with the velocity data. This is particularly evident for the Armona inlet, since several studies have shown the narrowing of this inlet during the last decades, which has led to a hydraulic efficiency loss (Vila-Concejo *et al.*, 2002; Pacheco *et al.*, 2010; Jacob *et al.*, 2013).

Figure 4.6 – Mean velocities in the Faro-Olhão inlet in the 2011 Autumn campaigns performed in spring tide (left) and neap tide (right). The positive values correspond to the flood period and the negative values correspond to the ebb period.

Figure 4.7 – Mean velocities in the Armona inlet in the 2011 Autumn campaigns performed in spring tide (left) and neap tide (right). The positive values correspond to the flood period and the negative values correspond to the ebb period.

Figure 4.8 – Mean velocities in the Olhão channel in the 2011 Autumn campaigns performed in spring tide (left) and neap tide (right). The positive values correspond to the flood period and the negative values correspond to the ebb period.

Figure 4.9 – Mean velocities in the Faro channel in the 2011 Autumn campaigns performed in spring tide (left) and neap tide (right). The positive values correspond to the flood period and the negative values correspond to the ebb period.

The results of the sea surface elevation and current velocities show that the application of the SCHISM 3D in barotropic mode in the Ria Formosa represents adequately the main circulation patterns in the lagoon.

5. Implementation of the baroclinic model

5.1 Data for the model validation

The validation of the model was performed by comparing the computed time series with sea surface elevation, temperature and salinity data from three seasonal campaigns performed in 2017 in the scope of project UBEST (Cravo *et al.*, 2017a, b, c). In these campaigns seven stations were selected to cover all the water bodies (WB) established for the Ria Formosa (Figure 2.1). *In situ* measurements of temperature and salinity were made simultaneously at each station, every two hours during a complete semidiurnal tidal cycle (~ 12.5 h), using YSI multiparametric probes. Four pressure transducers (PT) were also installed in different sites, to measure the sea surface elevation and water temperature every 10 minutes (Figure 2.1). Additionally, *in-situ* data were used from the Real-Time Observatory station installed in the main channel of the western sector of the Ria Formosa (Figure 2.1), which measured continuously water temperature and salinity with 15 minutes intervals. The coordinates of the field stations and the sampling periods for the three campaigns are indicated in Table 5.1.

Table 5.1 – Coordinates of the stations and the sampling periods corresponding to the field campaigns performed in 2017 and to the Real-Time Observatory station.

Station	WB	Latitude	Longitude	Period of sampling		
				May	September	October
Real-Time Observatory (RTO)	WB2	37.002755	-7.921182	26 – June 2	3 – 21	3 – 27
1 – Bridge of Faro Beach	WB1	37.009001	-7.993699	30, 08:16 – 21:07	14, 07:00 – 21:30	25, 07:00 – 20:15
2 – Faro Commercial Port	WB2	37.002754	-7.921186	30, 07:26 – 20:25	14, 07:30 – 20:40	25, 07:40 – 21:20
3 – Fuzeta	WB4	37.050767	-7.742030	30, 07:00 – 19:35	14, 07:00 – 20:00	25, 07:00 – 20:00
4 – Tavira	WB5	37.116308	-7.628722	30, 07:39 – 20:15	14, 07:00 – 20:00	25, 07:00 – 20:00
5 – Cacela	WB5	37.153973	-7.553397	30, 06:54 – 19:25	14, 07:00 – 20:00	25, 07:02 – 20:00
6 – Olhão channel	WB3	36.998081	-7.841326	31, 07:45 – 20:45	15, 07:00 – 19:50	26, 07:00 – 20:40
7 – Faro-Olhão inlet (Boundary Sation)	WB3	36.971926	-7.871217	31, 08:50 – 21:45	15, 07:40 – 20:25	26, 07:40 – 20:10
PT1 – Bruce's Yard	WB2	37.021122	-7.945661	29 – June 1	12 – 21	23 – 27
PT2 – Faro Commercial Port	WB2	37.002755	-7.921182	25 – June 2	11 – October 3	23 – November 1
PT3 – Deserta Island Pier	WB3	36.965858	-7.871014	24 – June 1	11 – 18	23 – 31
PT4 – Quatro Águas de Tavira	WB5	37.115725	-7.629700	26 – June 2	8 – 22	24 – 31

5.2 Model validation

5.2.1 Model setup

To implement SCHISM in baroclinic mode, the grid and the bathymetry were updated for the 2017 conditions. Regarding the grid resolution, some areas were refined, such as Cacela, Fuzeta, Armona and Ancão inlets, and some channels (Faro channel, from the Faro Commercial Port to the Bruce's Yard, and Faro beach channel) and the Gilão River was introduced in the domain. Additionally, the ocean part of the domain was extended due to instabilities in the current velocity simulations at the edges of the domain. The final grid used in the validation of the baroclinic model was characterized horizontally by 98308 nodes and 192824 elements (Figure 5.1). The bathymetric information from 1980 to 2010 was updated with the topographic and bathymetric surveys performed during 2011, along the Portuguese coast with LiDAR equipment (Light Detection And Ranging) (Silva *et al.*, 2012). The use of airborne LiDAR is an important innovation, especially in areas like the Ria Formosa, where the extension of the area and access limitations make it difficult and expensive to use traditional bathymetric methods. This is an important dataset, with great detail and accuracy (resolution of 2 meters). This information was combined with the existing bathymetry, since the data obtained with LiDAR equipment are limited to a coastal band with an approximate width of 1 km. Additionally, the bathymetry in the upstream area of the Gilão River was developed based on local knowledge and unpublished works, given the scarcity of bibliographic information (Figure 5.1).

Figure 5.1 – Horizontal grid and bathymetry (2011, MSL – mean sea level). Location of the sampling stations.

In the validation process, the model was forced by: i) tides, temperature and salinity at the oceanic boundary; ii) river flow rate, temperature and salinity at the river boundary (Gilão river); and iii) atmospheric data (wind, atmospheric pressure, air temperature, specific humidity, downwards longwave and solar radiation) at the surface.

To define the oceanic boundary conditions (BC) of temperature, for each season, four tests were made:

i) constant value, obtained from the mean temperature recorded in the campaigns at the Boundary Station;
ii) constant value (for May, September and October 2017), estimated from the Iberian-Biscay-Irish Monitoring Forecasting Centre (IBI-MFC; http://marine.copernicus.eu/about-us/about-producers/ibi-mfc/);
iii) time varying temperature, from data recorded by the Deserta Island PT;
iv) time and space varying salinity and temperature from the Iberian-Biscay-Irish Monitoring Forecasting Centre (IBI-MFC; http://marine.copernicus.eu/about-us/about-producers/ibi-mfc/).

To define the conditions at the river boundary, the APA website (National Water Resources database) (https://snirh.apambiente.pt/) was accessed to obtain data from the Bodega Hydrometric Station, which is located in the Gilão River basin. The river flow rate and the temperature were set based on climatology estimated from data available in the APA website. For salinity, the boundary conditions were constant and defined as 0 in the river and 36.5 in the ocean boundary. The boundary conditions of temperature, salinity and river flow tested for the open boundaries and for each season are presented in Table 5.2.

Table 5.2 – Boundary conditions of temperature, salinity and river flow rate for the oceanic and river boundaries. The values of temperature in bold corresponds to the values obtained from the IBI-MFC.

Boundary	Campaign	Variable		
		T (ºC)	Salinity	Flow rate (m^3/s)
Ocean	May 2017	19.3/**19.1**	36.5	-
	September 2017	19.2/**22.1**	36.5	-
	October 2017	20.6/**22.2**	36.5	-
River	May 2017	20.2	0	0.38
	September 2017	22.8	0	0.03
	October 2017	20.5	0	0.20

The atmospheric dataset used in the simulations was the ERA-Interim (Dee *et al.*, 2011) produced by the European Centre for Medium-Range Weather Forecasts (ECMWF; https://www.ecmwf.int/). This dataset is a global atmospheric reanalysis from 1979 to August 2017.

5.2.2 Results

Figure 5.2 to Figure 5.5 present the comparison between the sea surface elevation from the field campaigns and the results from the simulations. The model fits very well the hydrodynamic circulation within the lagoon (Figure 5.2, Figure 5.3 and Figure 5.5) and in the external area (Figure 5.4). In Table 5.3 the RMSE for the sea surface elevation is presented for the same stations. The RMSE at Bruce station ranged from 7 to 8 cm, at Faro Commercial Port from 5 to 7 cm, at Deserta Island from 6 to 8 cm and at Tavira from 5 to 9 cm. These results suggest that the implementation of the SCHISM 3D model in baroclinic mode slightly improved the performance of the model in representing the hydrodynamic circulation, since the RMSE from the barotropic to baroclinic mode decreased. In spite of this improvement, differences still exist between the time series computed and the field data, partly because the bathymetric data are not contemporaneous with the field campaigns periods.

Table 5.3 – RMSE (cm) between the sea surface elevation recorded by the four PT (Bruce, Faro Commercial Port, Deserta Island and Tavira) and the baroclinic simulations for the campaigns performed in May, September and October 2017 in the Ria Formosa.

PT	Bruce			Faro Commercial Port			Deserta Island			Tavira		
Campaign	M	S	O	M	S	O	M	S	O	M	S	O
RMSE	0.07	0.08	0.07	0.07	0.05	0.06	0.06	0.08	0.08	0.05	0.08	0.09

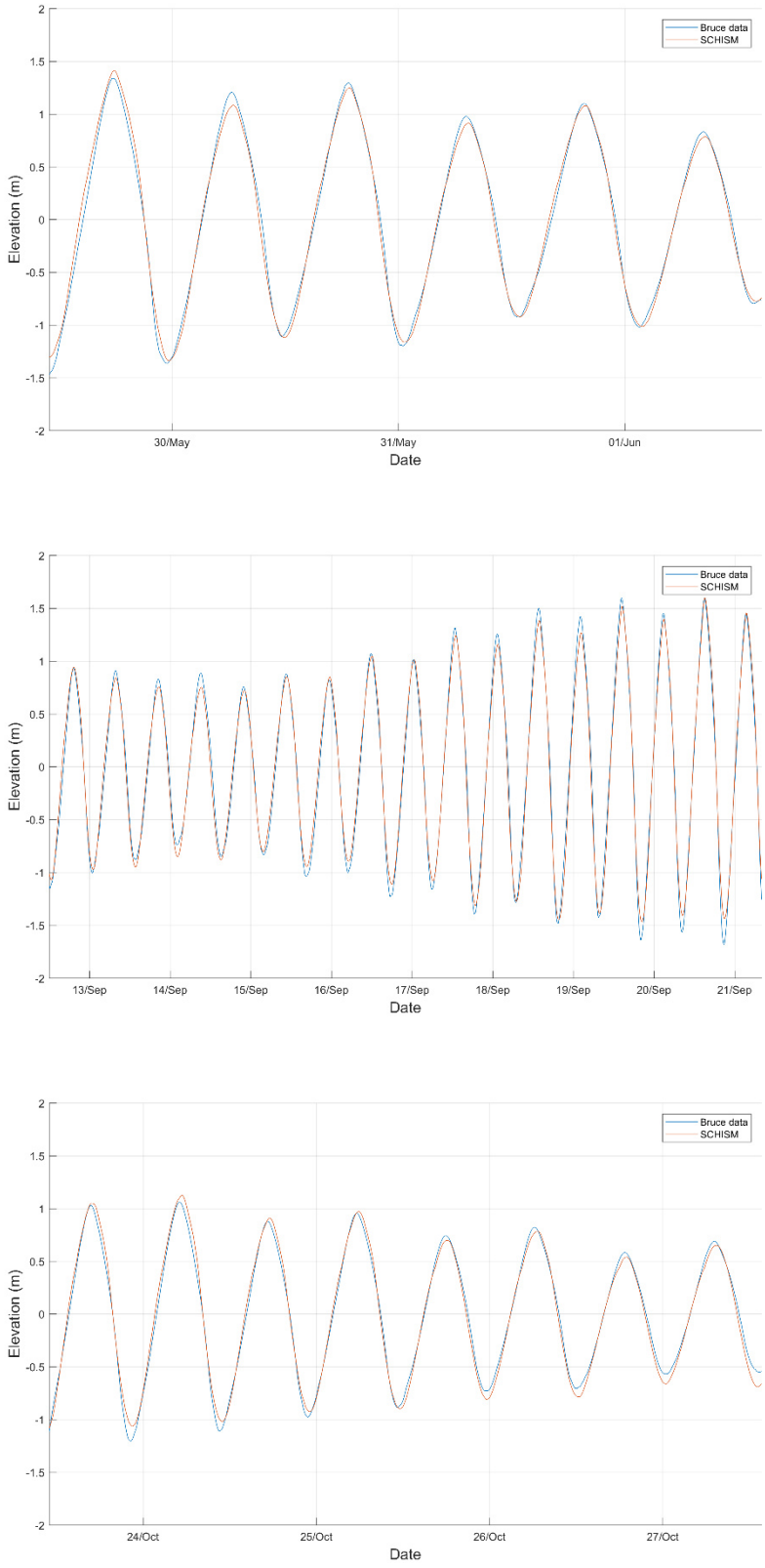

Figure 5.2 – Comparison between the temporal series of the sea surface elevation (m) recorded by the Bruce Yard PT and the results of the model for the campaigns performed in May, September and October.

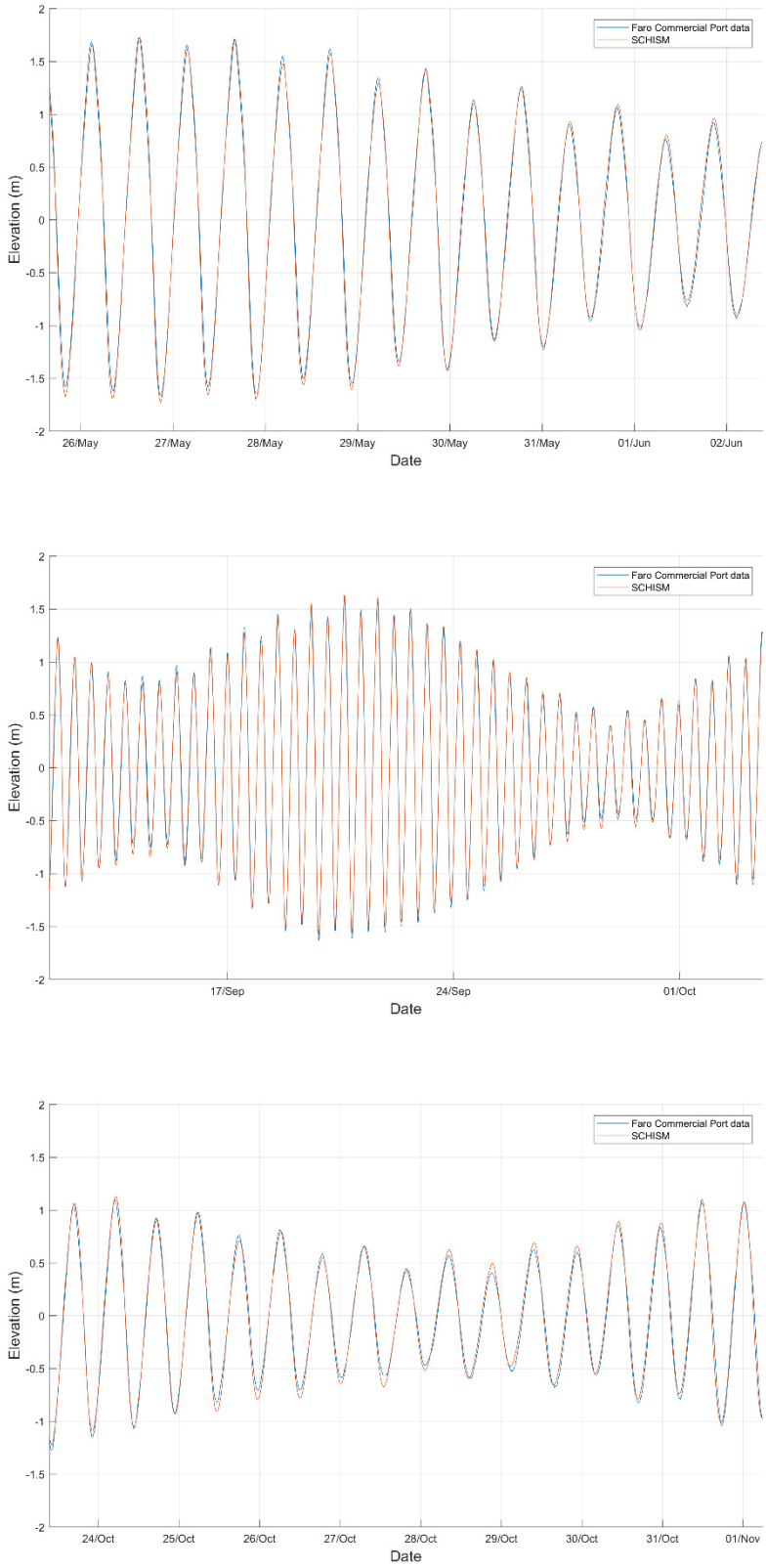

Figure 5.3 – Comparison between the temporal series of the sea surface elevation (m) recorded by the Faro Commercial Port PT and the results of the model for the campaigns performed in May, September and October.

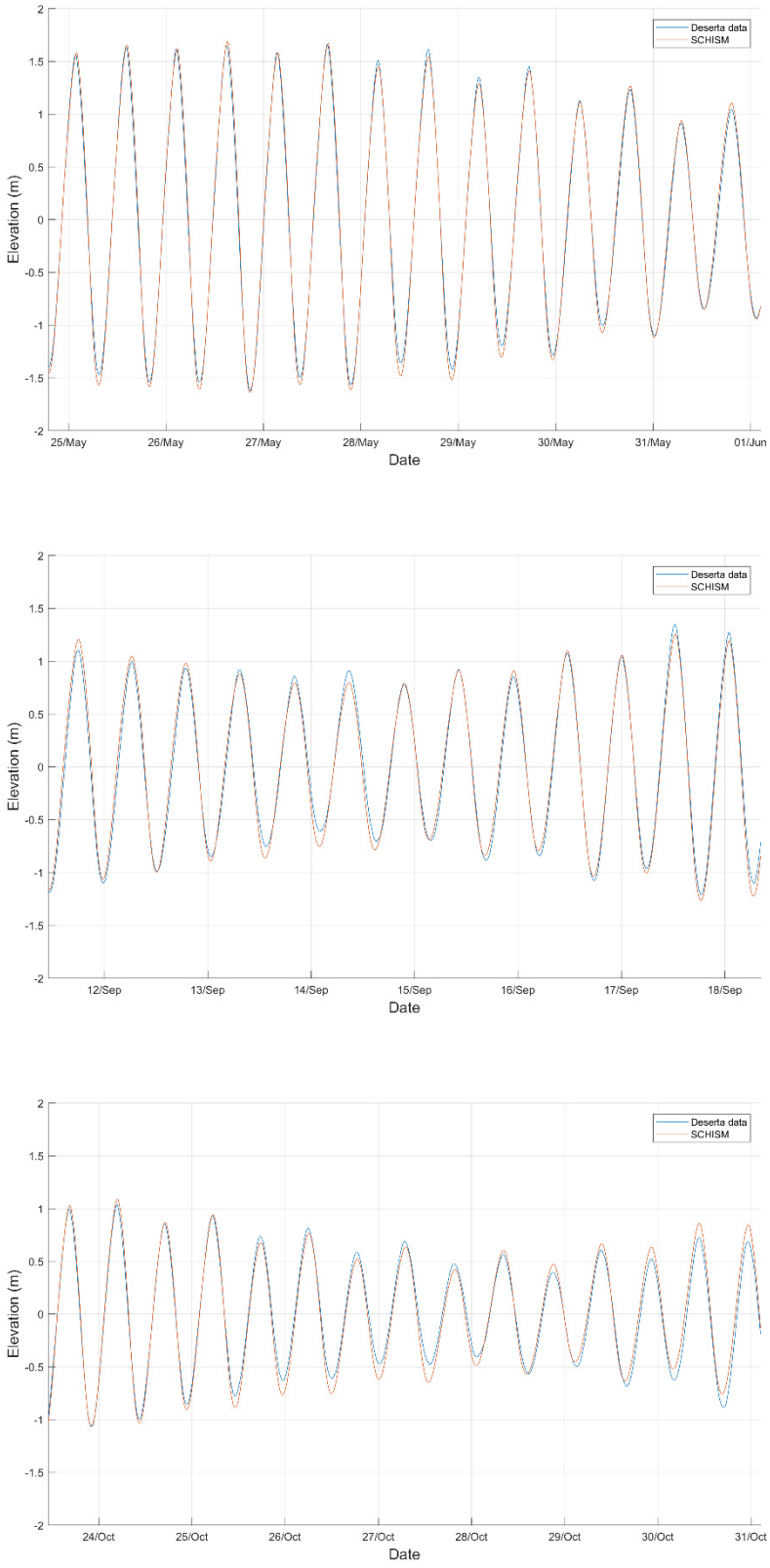

Figure 5.4 – Comparison between the temporal series of the sea surface elevation (m) recorded by the Deserta PT and the results of the model for the campaigns performed in May, September and October.

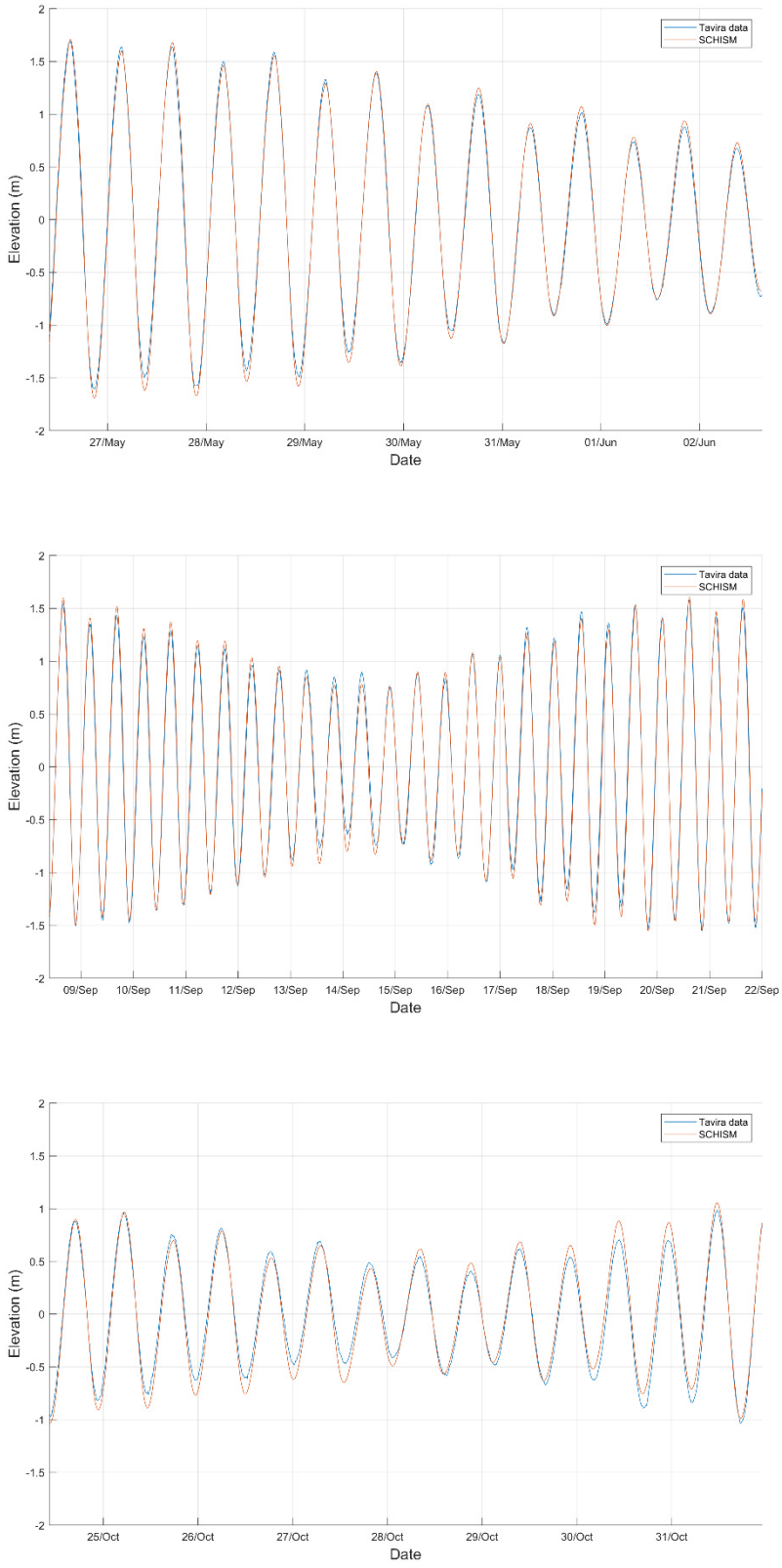

Figure 5.5 – Comparison between the temporal series of the sea surface elevation (m) recorded by the Tavira PT and the results of the model for the campaigns performed in May, September and October.

Regarding temperature and salinity, the RMSE for the several simulations is shown in Figure 5.6 and Figure 5.7, respectively. Globally, and for the two variables, the highest values of RMSE are found in the stations located at the edges of the lagoon (1-Bridge of Faro Beach and 5-Cacela). For temperature, the best results for the campaigns performed in May and October were found in the simulation using the BC constant as the mean of the field campaign. However, in September, the best scenario was obtained using the constant value from the IBI-MFC. This campaign showed to have higher values of RMSE, which can be associated with an upwelling event that prevailed during the campaign period. This process upwelled cold water responsible for the water temperature decrease at the Boundary Station, which was not so intense in the stations located within the lagoon. This means that, if the model is forced by the value registered at the Boundary Station during the campaign (19.2 ºC), the RMSE values are lower in this station, but higher in the remaining stations. However, if the model is forced by the constant value estimated from the IBI-MFC (22.1 ºC), the RMSE is higher in the Boundary Station and lower in the stations inside the lagoon.

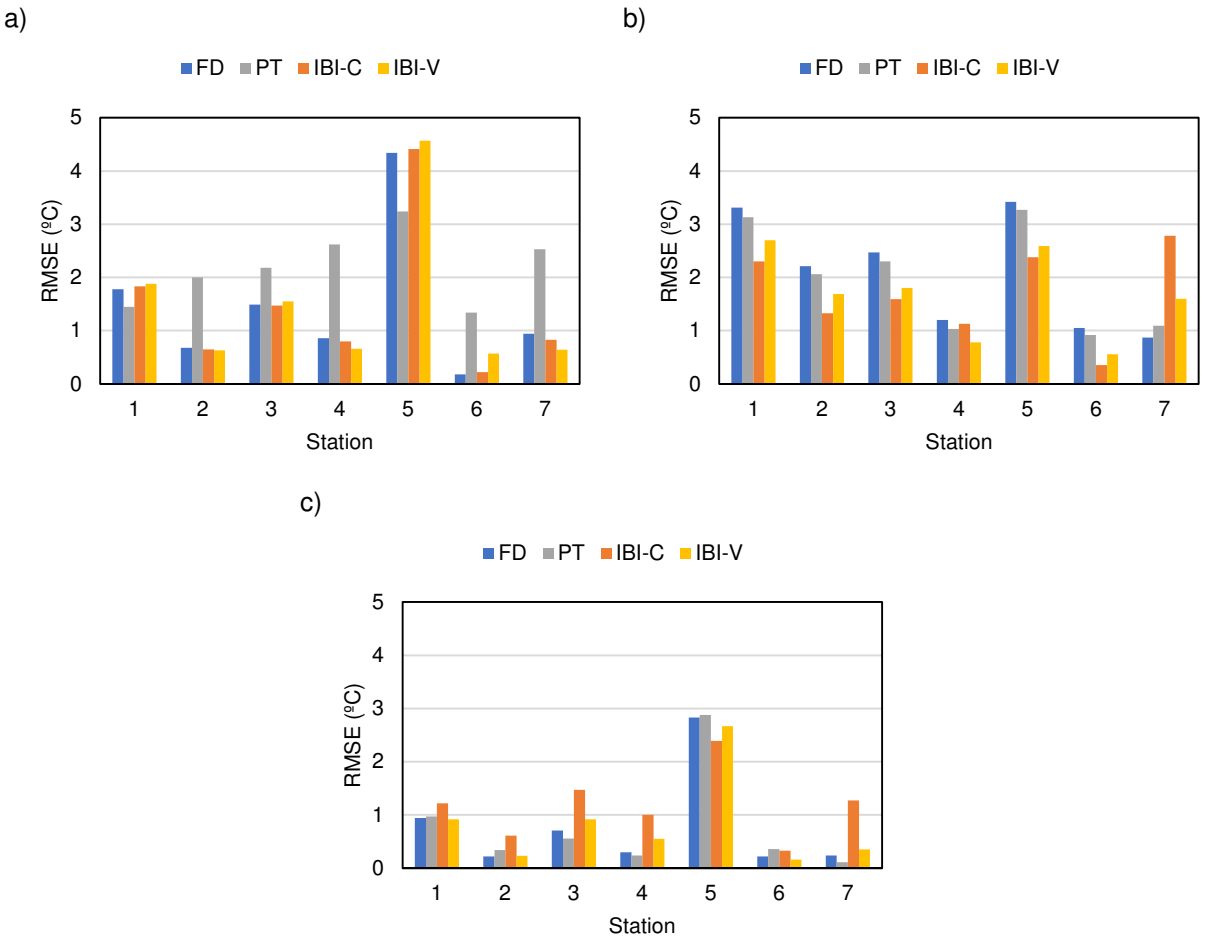

Figure 5.6 – RMSE (ºC) between the water temperature registered during the seasonal campaigns with the baroclinic simulations of the model for the campaigns performed in May (a), September (b) and October (c) 2017 in the Ria Formosa using four different boundary conditions: data measured at BS during the field campaigns (FD); data measured by the Deserta Island PT (PT); constant values (IBI-C) and time and space varying values (IBI-V) from IBI-MFC.

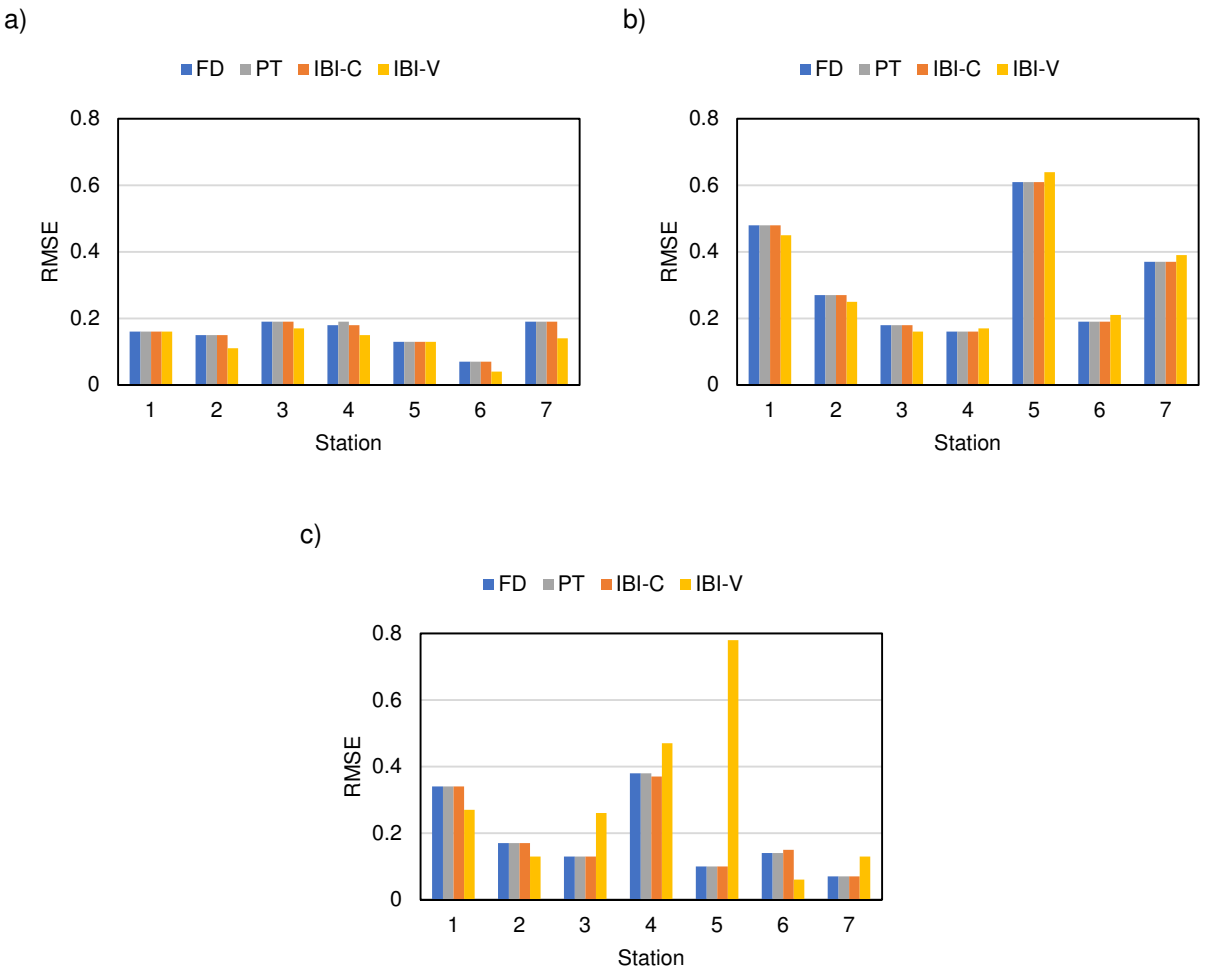

Figure 5.7 – RMSE between the salinity registered during the seasonal campaigns with the baroclinic simulations of the model for the campaigns performed in May (a), September (b) and October (c) 2017 in the Ria Formosa using four different boundary conditions: data measured at BS during the field campaigns (FD); data measured by the Deserta Island PT (PT); constant values (IBI-C) and time and space varying values (IBI-V) from IBI-MFC.

Thus, given the high values of RMSE obtained in September using the constant value from the field campaign, the best scenario for the three field campaigns is using the BC constant from the IBI-MFC to force the model. In consequence, the comparison between the salinity and water temperature of the three campaigns and the simulations are presented and described below from the IBI-MFC simulations (BC constant). As additional information, the ANNEX section also presents the results from the several simulations.

The salinity at the seven stations, for the three campaigns, is presented in Figure 5.8 to Figure 5.14. Globally, the RMSE is lower than 0.6 (Figure 5.7) and the results show that the salinity in the Ria Formosa is higher than 36. The exception is at Tavira station, where the signal of the freshwater is visible, particularly in the May campaign. This variable seems to be mainly controlled by the boundary condition defined at the oceanic boundary, since no significant variations are observed in the model results. This fact is also supported by the results from the simulations using the BC variable from the IBI-MFC, which were very similar to the ones presented below (ANNEX I). Given these results and the

importance of evaporation in shallow ecosystems, this process must be considered and explored in future applications for a better representation of the salinity variability.

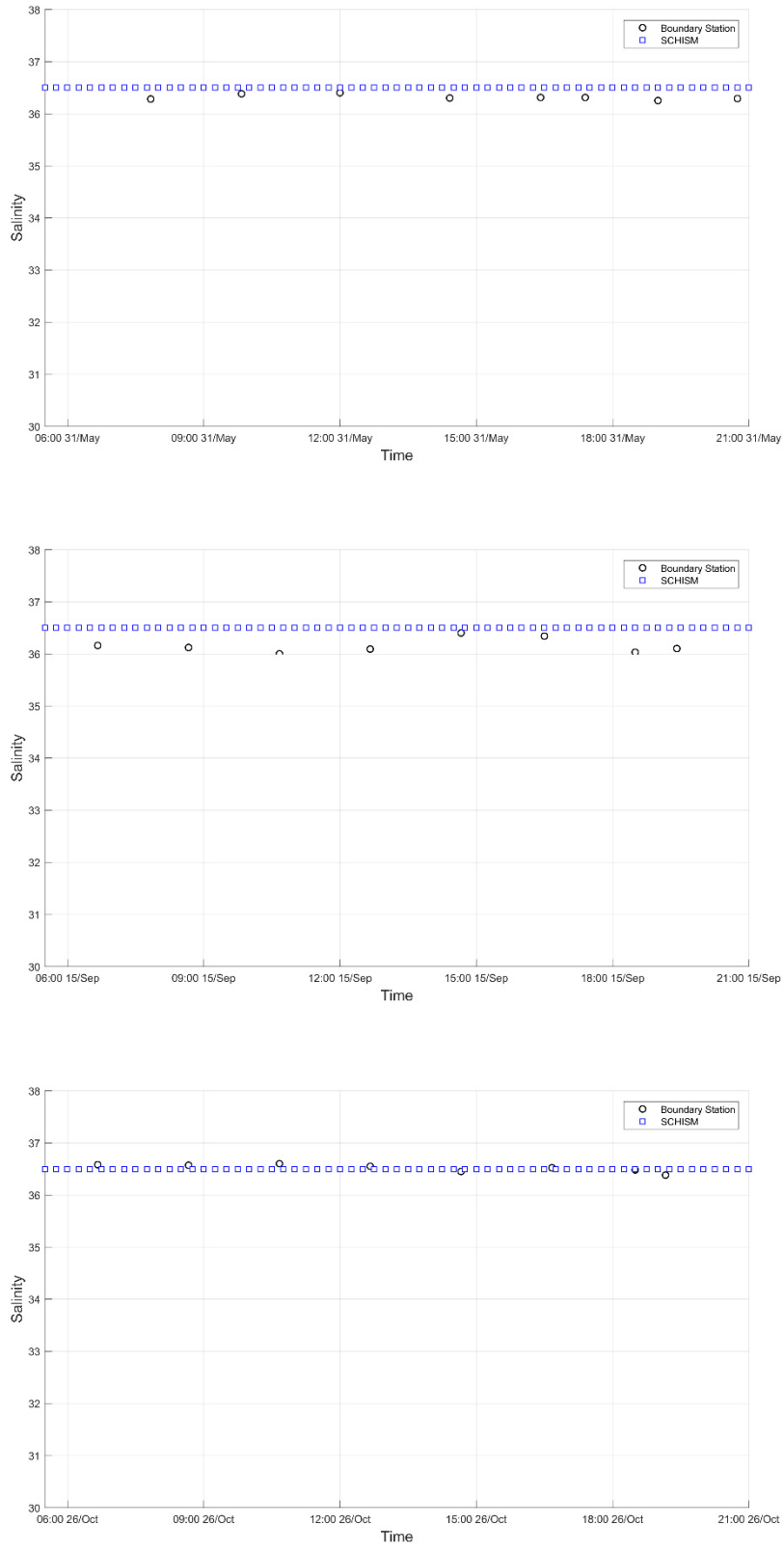

Figure 5.8 – Comparison between the temporal series of salinity recorded at the Boundary Station and the results of the model for the campaigns performed in May, September and October.

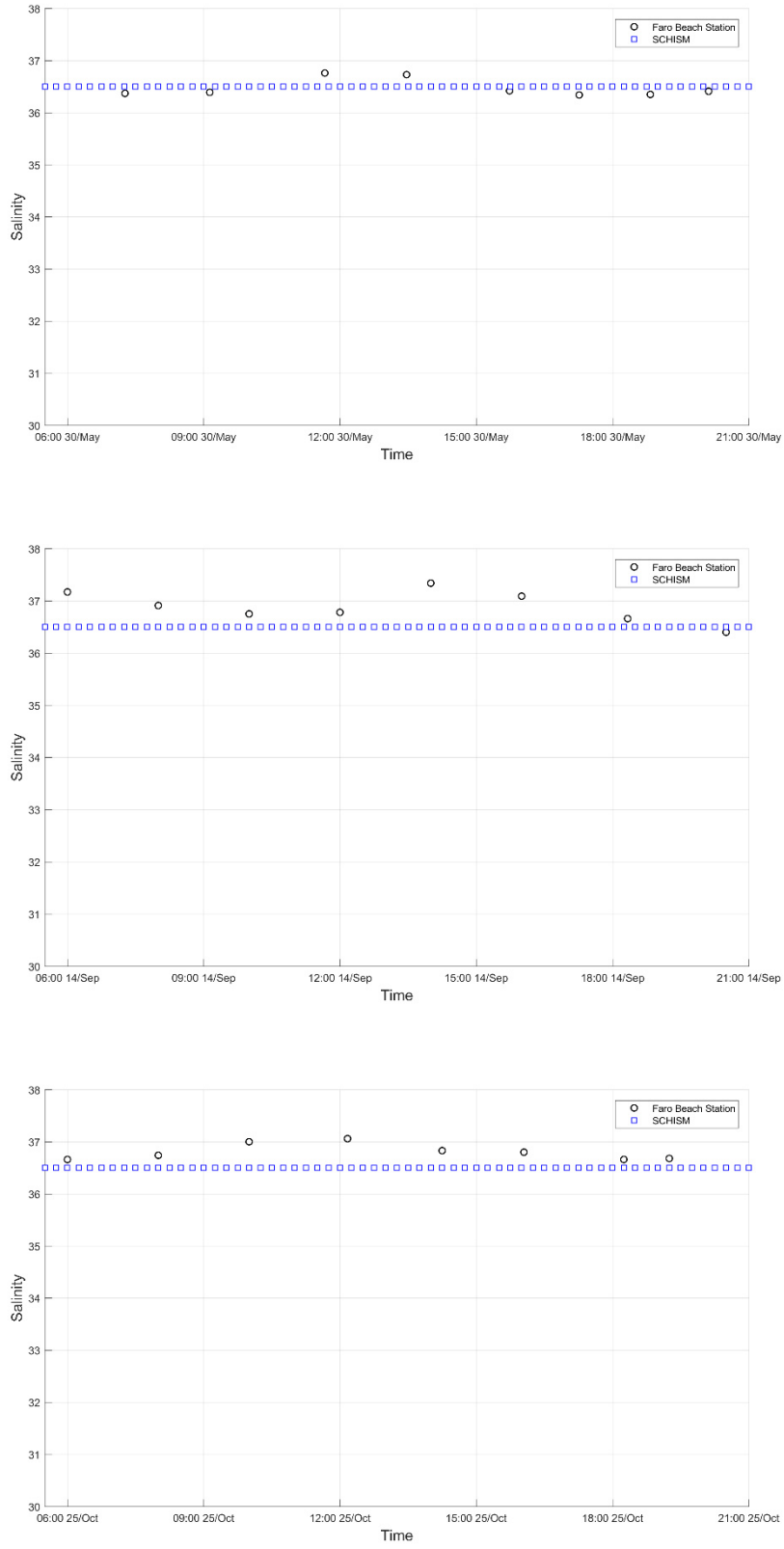

Figure 5.9 – Comparison between the temporal series of salinity recorded at Faro Beach station and the results of the model for the campaigns performed in May, September and October.

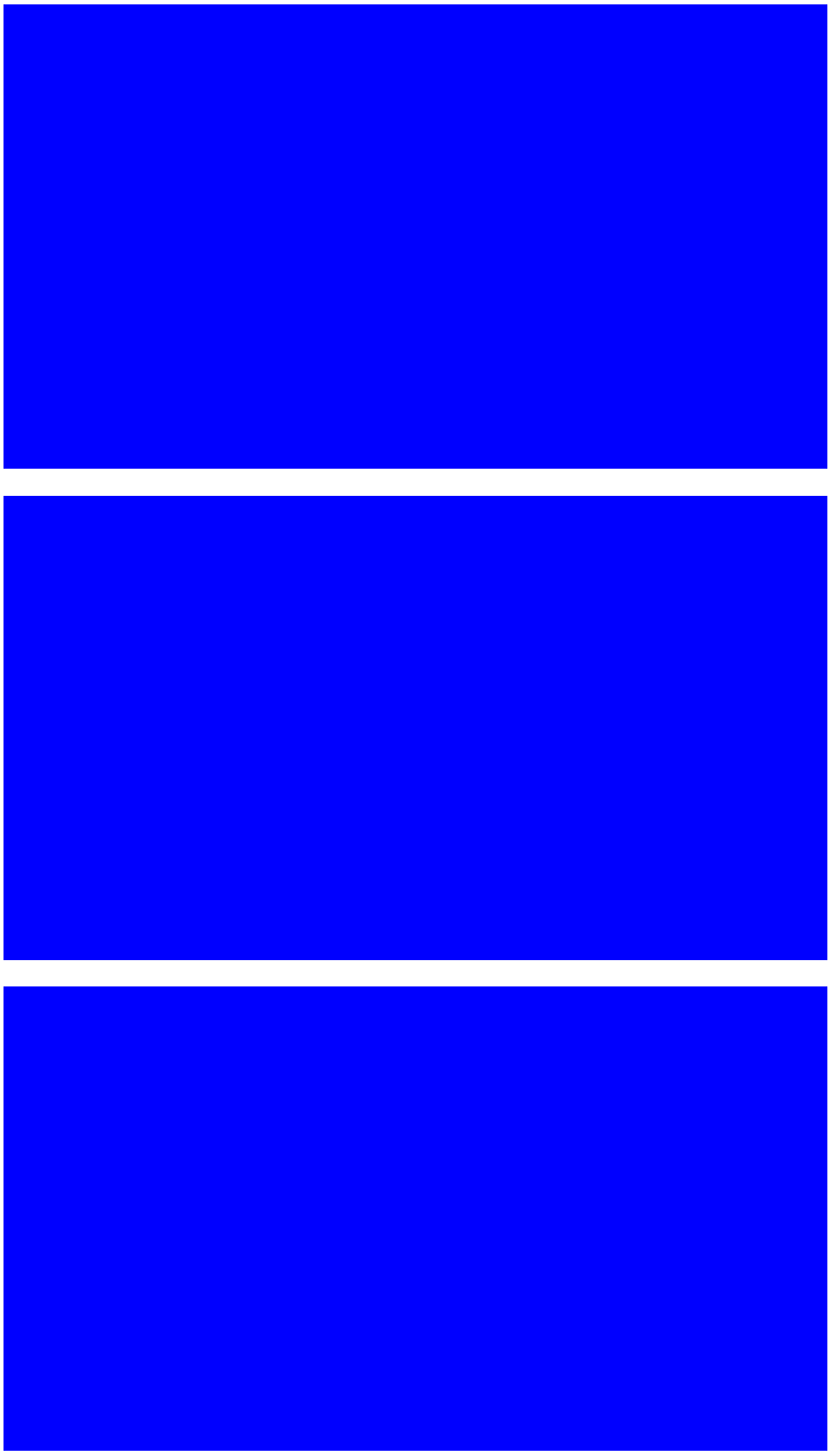

Figure 5.10 – Comparison between the temporal series of salinity recorded at Faro Commercial Port station and the results of the model for the campaigns performed in May, September and October.

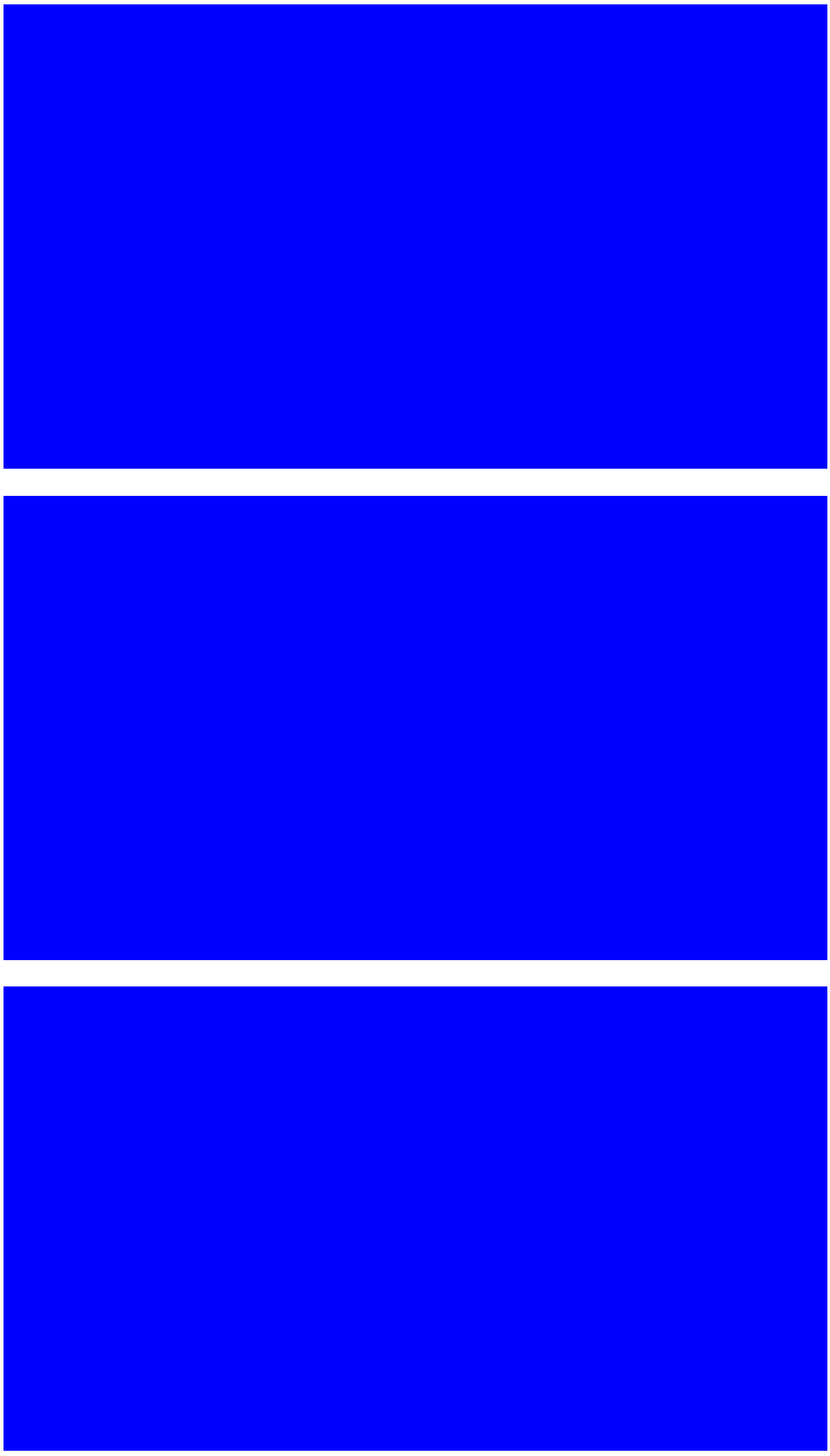

Figure 5.11 – Comparison between the temporal series of salinity recorded at Fuzeta station and the results of the model for the campaigns performed in May, September and October.

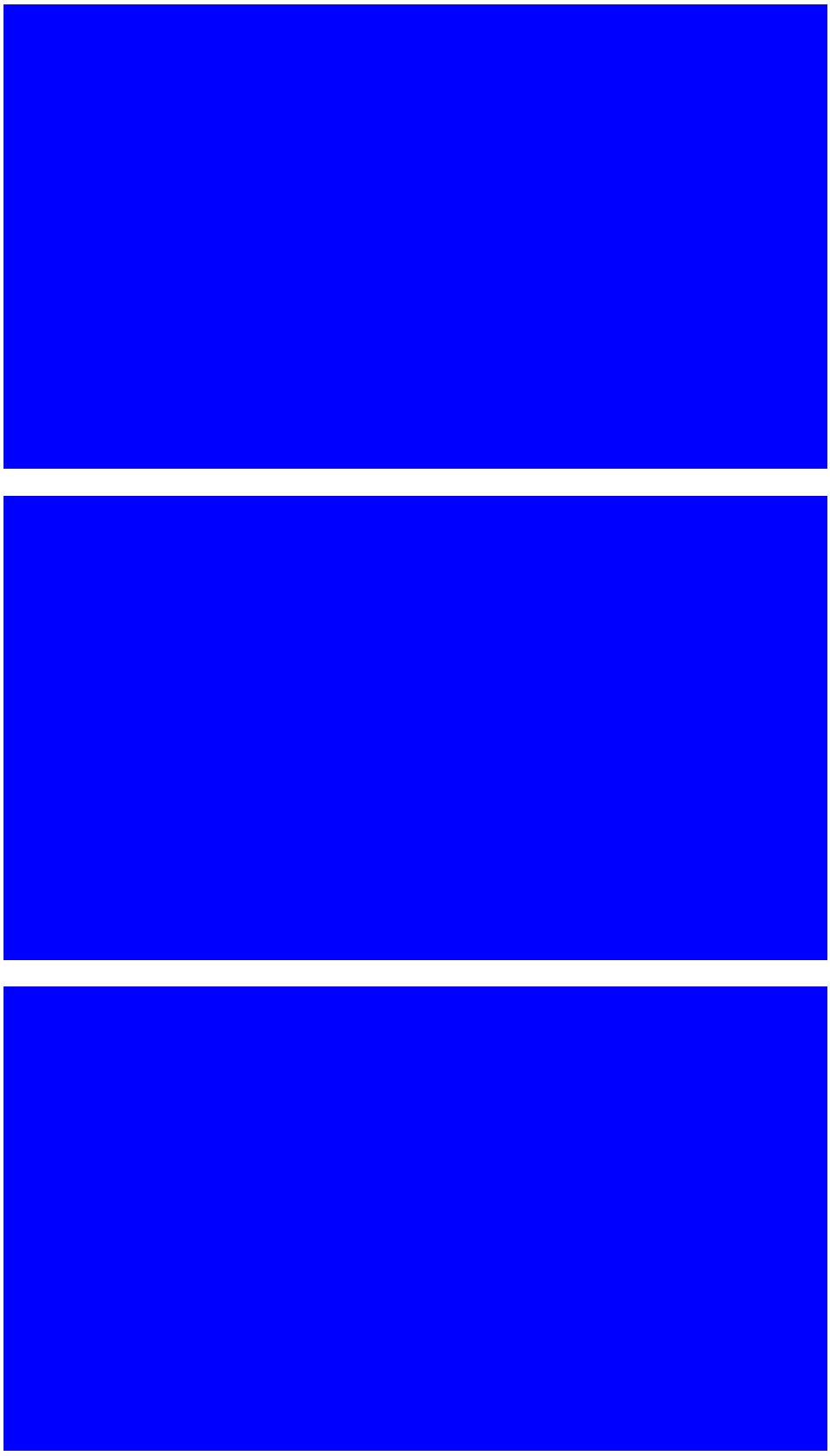

Figure 5.12 – Comparison between the temporal series of salinity recorded at Tavira station and the results of the model for the campaigns performed in May, September and October.

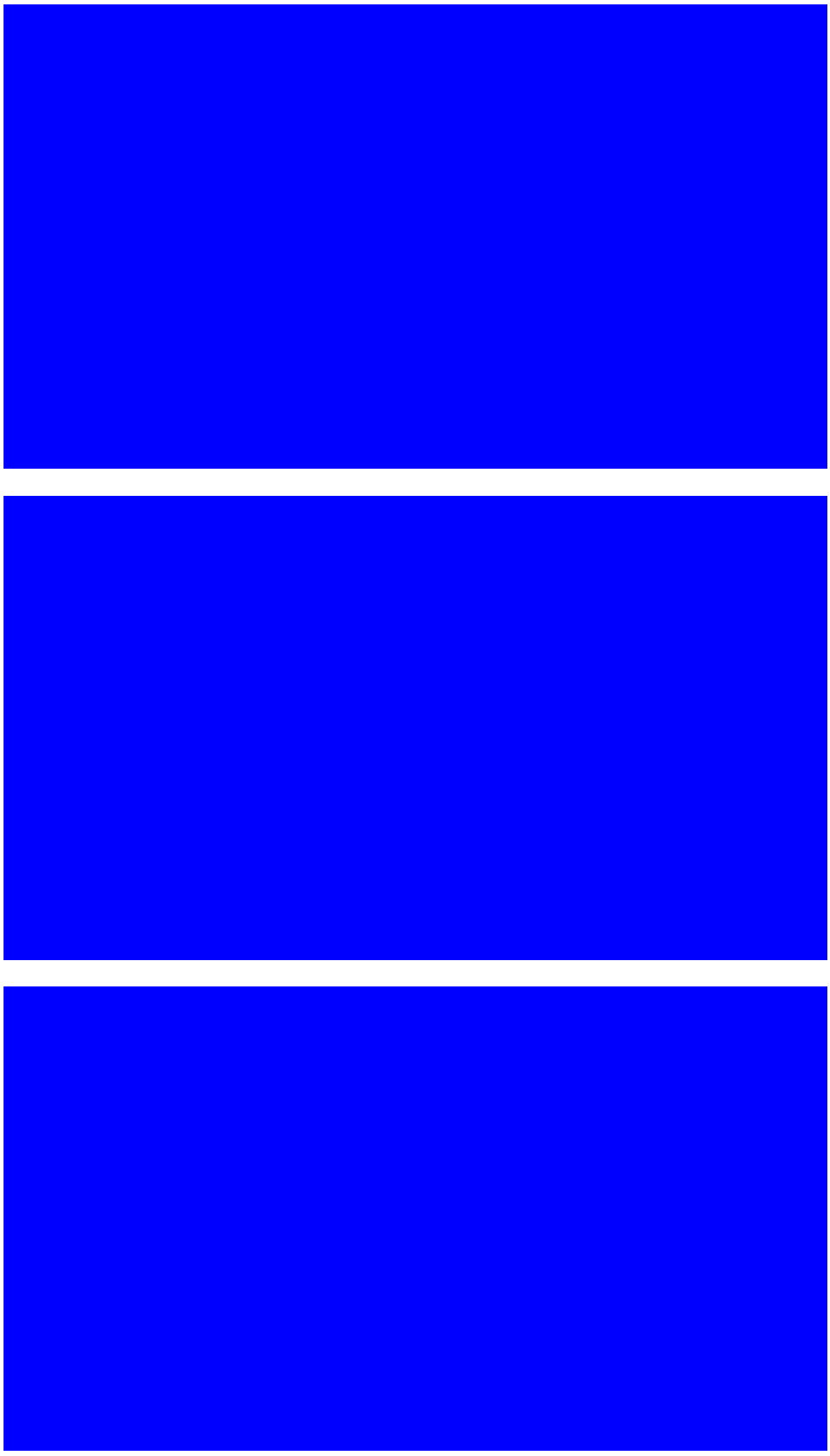

Figure 5.13 – Comparison between the temporal series of salinity recorded at Cacela station and the results of the model for the campaigns performed in May, September and October.

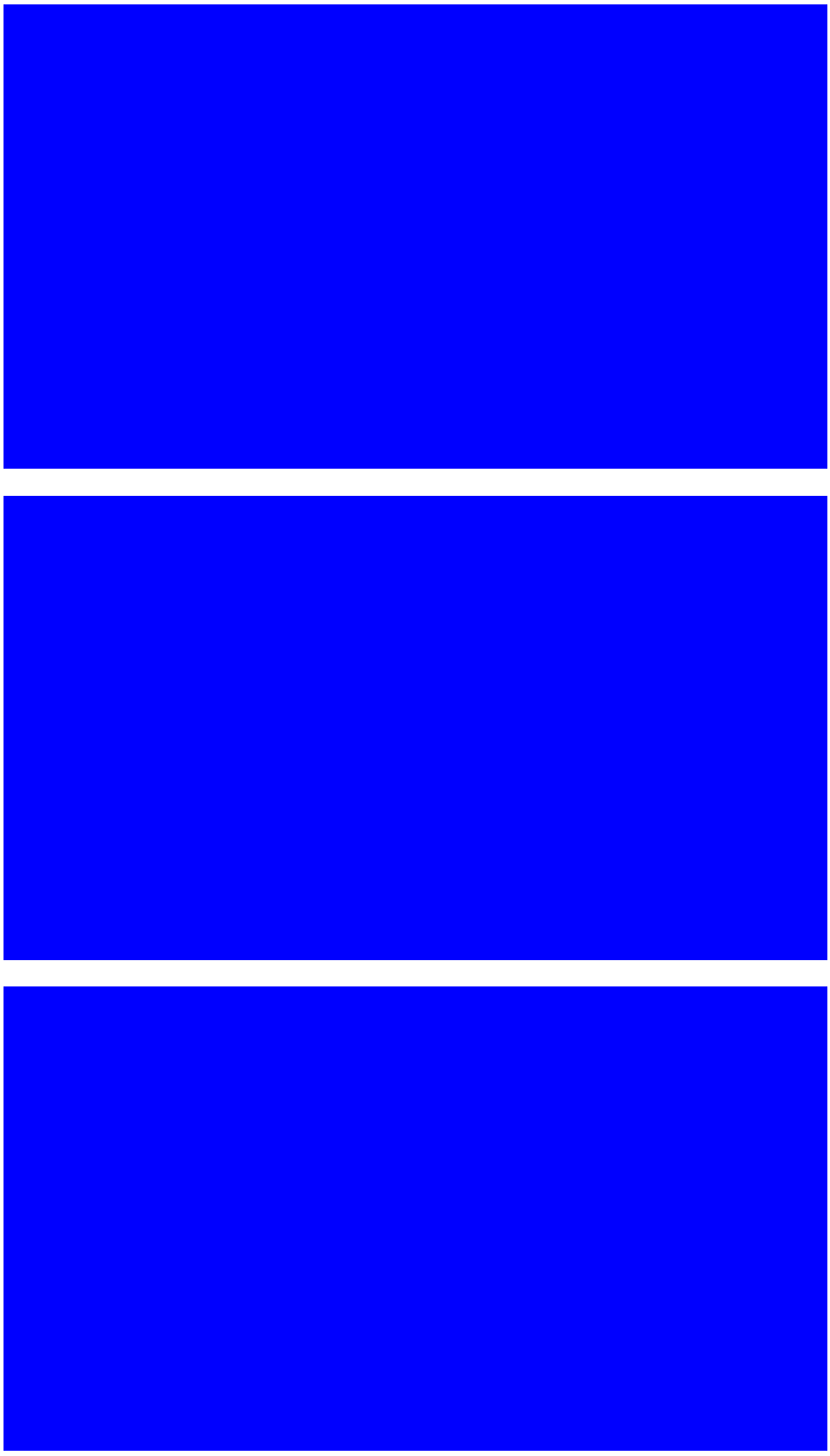

Figure 5.14 – Comparison between the temporal series of salinity recorded at Olhão Channel station and the results of the model for the campaigns performed in May, September and October.

Results for water temperature in all the stations and for the three seasons are presented in Figure 5.15 to Figure 5.22. Results show that the model is able to represent the main seasonal patterns and typically the RMSE are lower than 1ºC (Figure 5.6). However, there are some exceptions. Seasonally, the higher RMSE were obtained in the campaign performed in September, particularly at the Faro-Olhão inlet station (RMSE=2.8ºC). Spatially, the stations located at the edges of the lagoon (Bridge of Faro Beach and Cacela stations, RMSE ranges 1.2ºC-2.3ºC and 2.4ºC-4.4ºC, respectively), and also some inner areas (Fuzeta and Faro Commercial Port stations, RMSE ranges 1.5ºC-1.6ºC and 0.6ºC-1.3ºC, respectively) are the regions where the model usually underestimates the water temperature. One reason that may explain these differences is the shallowness of these areas and the composition of the bottom sediments (mostly mud). This is the case of Cacela, where water depth can be less than 20 cm at low tide. Thus, processes of heat transfer from the bottom sediments (heated when dry and exposed directly to the air and solar radiation during low tide) to the water column may be responsible for the increase in water temperature observed in this station. These processes are not reproduced by the model and may justify the higher RMSE at those stations. In the remaining stations (Olhão Channel and Tavira, RMSE ranges 0.2ºC-0.4ºC and 0.8ºC-1.1ºC, respectively) the RMSE are lower. Additionally, the results from the simulation using the BC variable from the IBI-MFC (ANNEX II) were very similar with the ones presented below, which supports the fact that the model underestimates the water temperature of this coastal lagoon and is not related to BC being constant.

Regarding to the Real-Time Observatory station (Figure 5.18), the results for May show that the model represents very well the temperature field in the first three days, but tends to underestimate in the remaining period (RMSE=0.8ºC). Regarding to September, the Real-Time Observatory station recorded the water temperature decrease between September 9 and 13, associated with the upwelling event. However, the small temperature increase observed after this period was underestimated by the model (RMSE=2.3ºC), also verified in the simulation forced by a variable BC (ANNEX II). The simulation of the last campaign demonstrated that the model reproduces very well the temperature field (RMSE=0.8ºC), when the solar radiation is not so intense. This behavior supports the hypothesis that in shallow systems, such as the Ria Formosa, the water temperature is not only controlled by the tidal propagation, the river flow and the heat exchanges at the surface, but also by other processes (e.g. heat transfer from the bottom sediments to the water column).

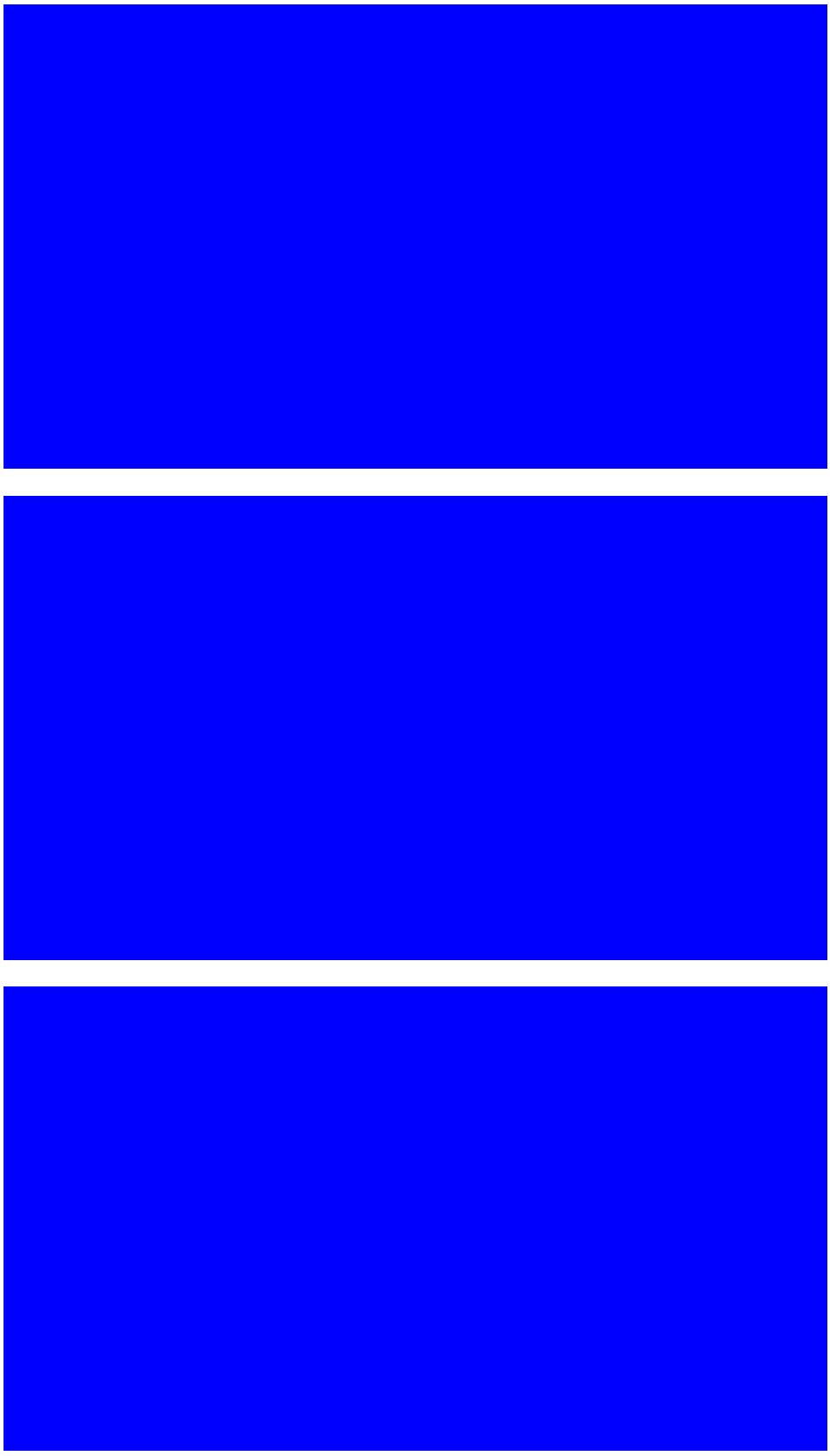

Figure 5.15 – Comparison between the temporal series of temperature recorded at the Boundary Station and the result of the model for the campaigns performed in May, September and October.

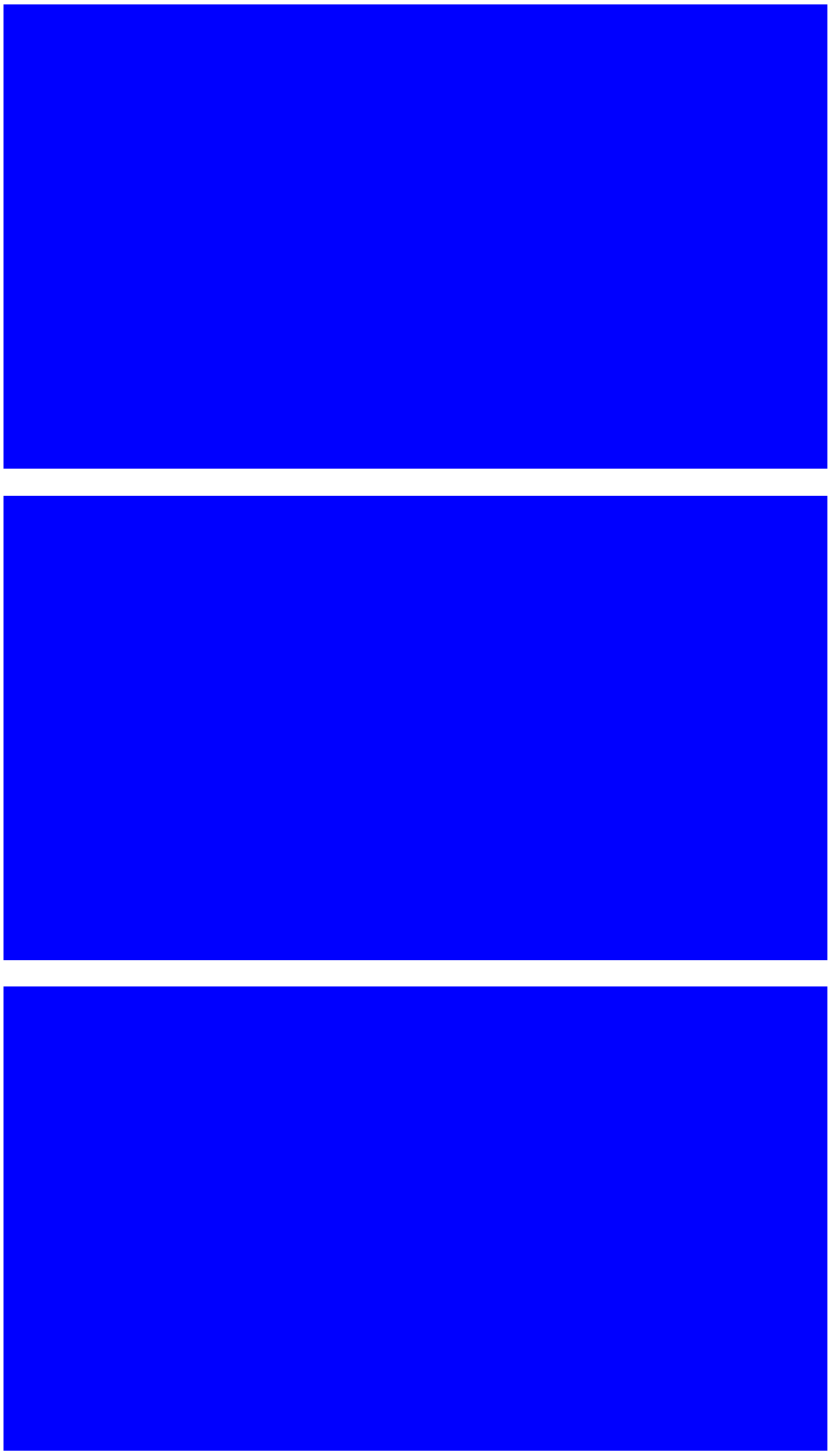

Figure 5.16 – Comparison between the temporal series of temperature recorded at Faro Beach station and the results of the model for the campaigns performed in May, September and October.

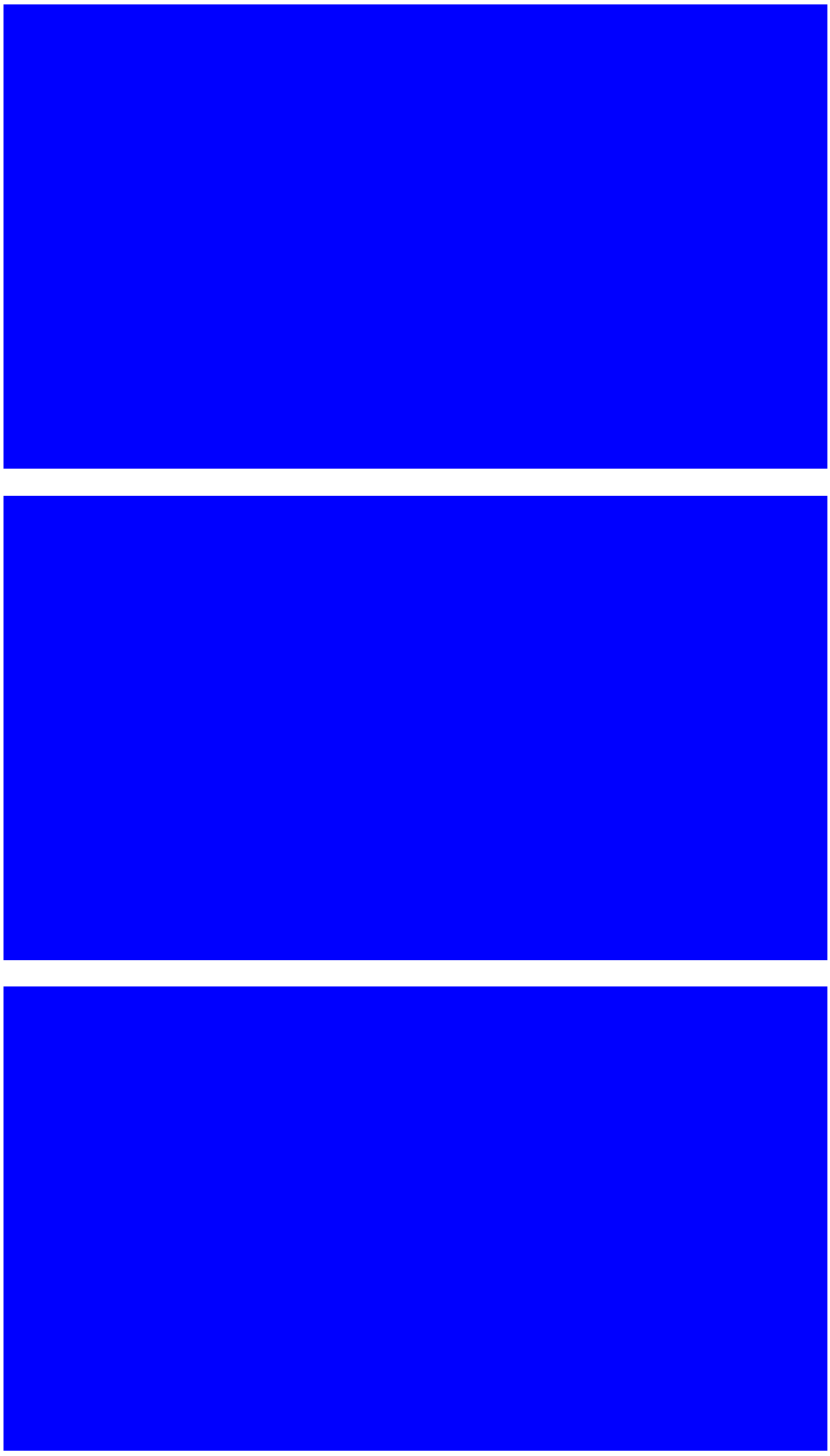

Figure 5.17 – Comparison between the temporal series of temperature recorded at Faro Commercial Port station and the results of the model for the campaigns performed in May, September and October.

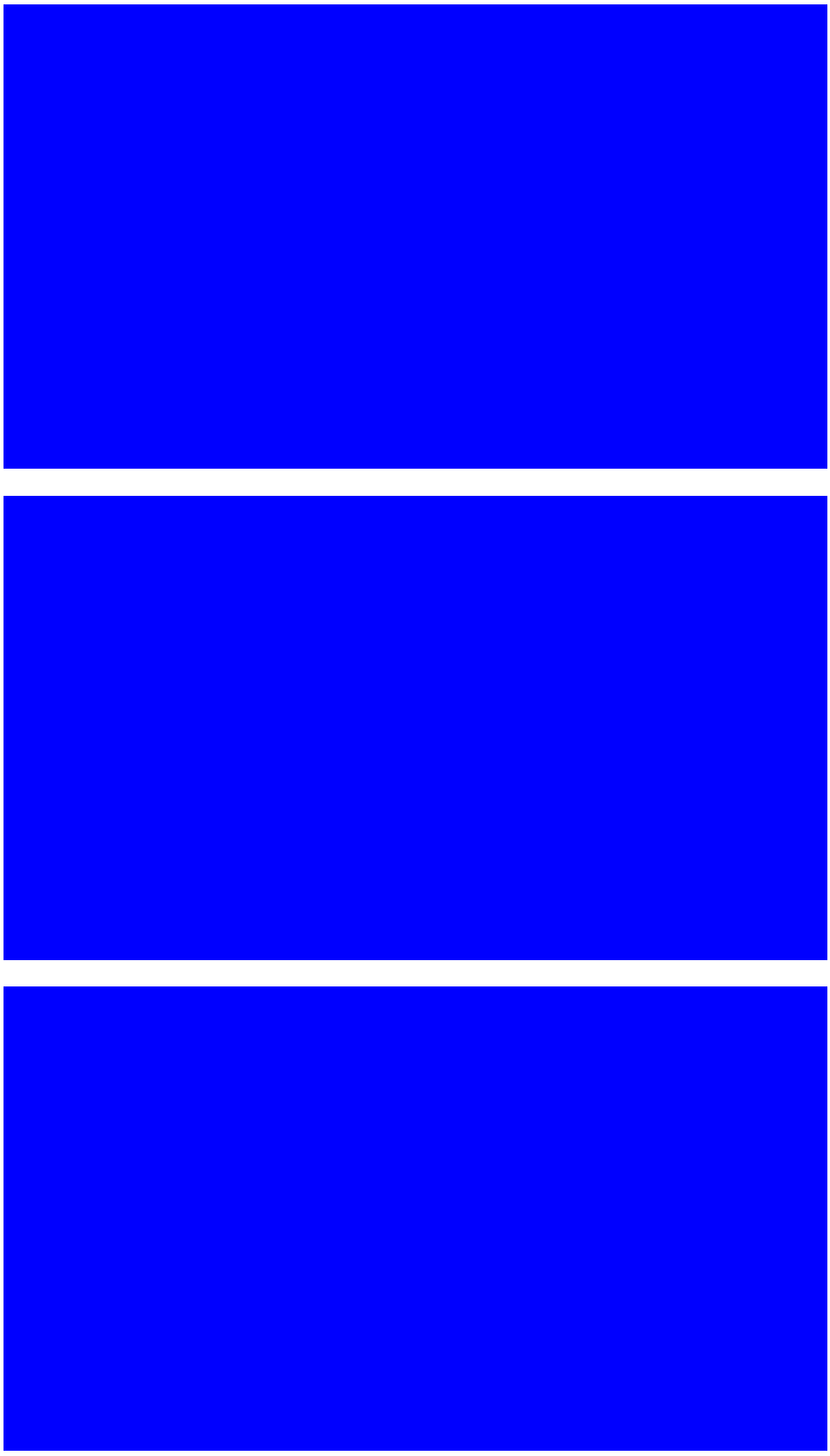

Figure 5.18 – Comparison between the temporal series of temperature recorded at Real-Time Observatory station and the results of the model for the campaigns performed in May, September and October.

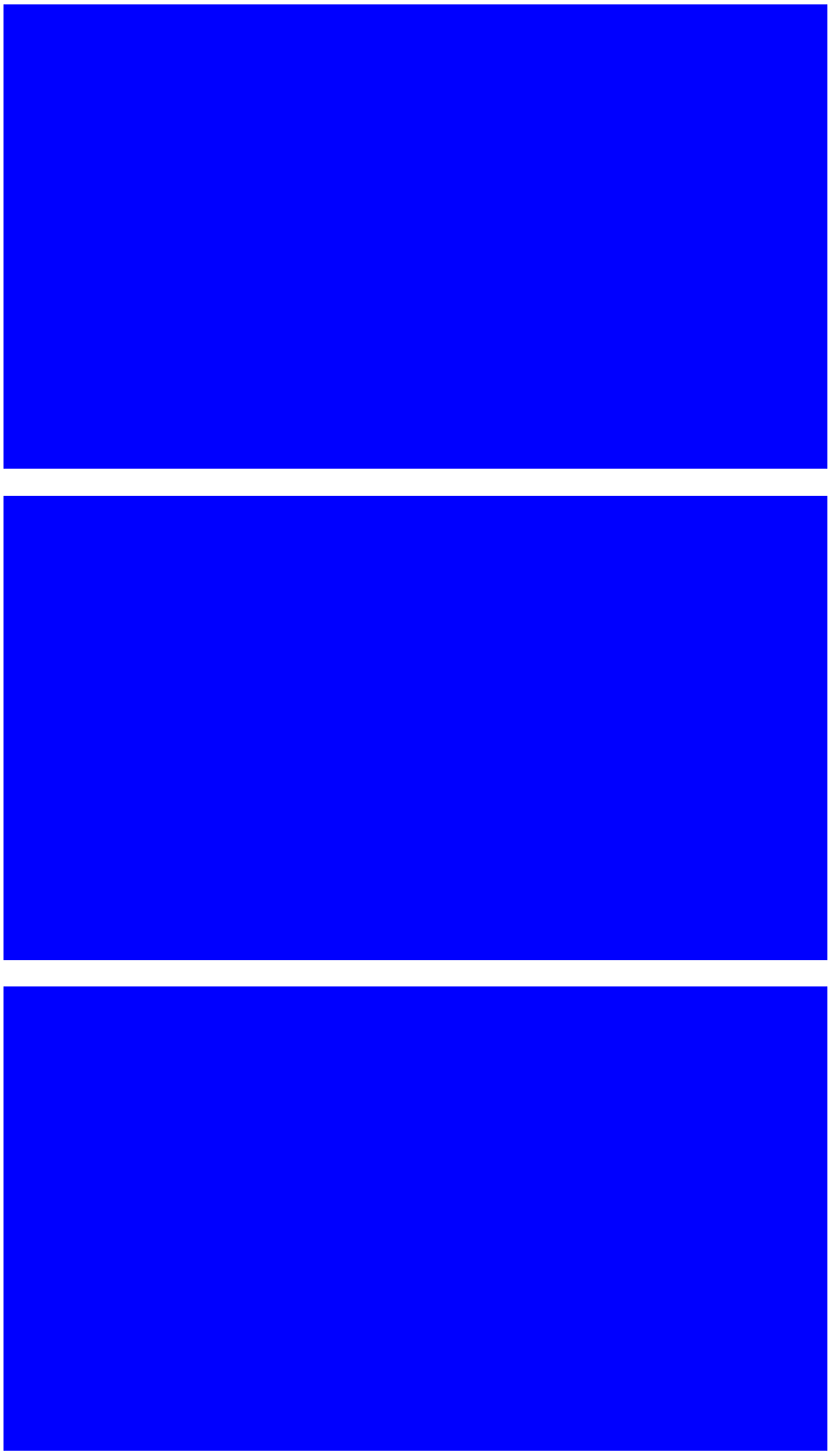

Figure 5.19 – Comparison between the temporal series of temperature recorded at Fuzeta station and the results of the model for the campaigns performed in May, September and October.

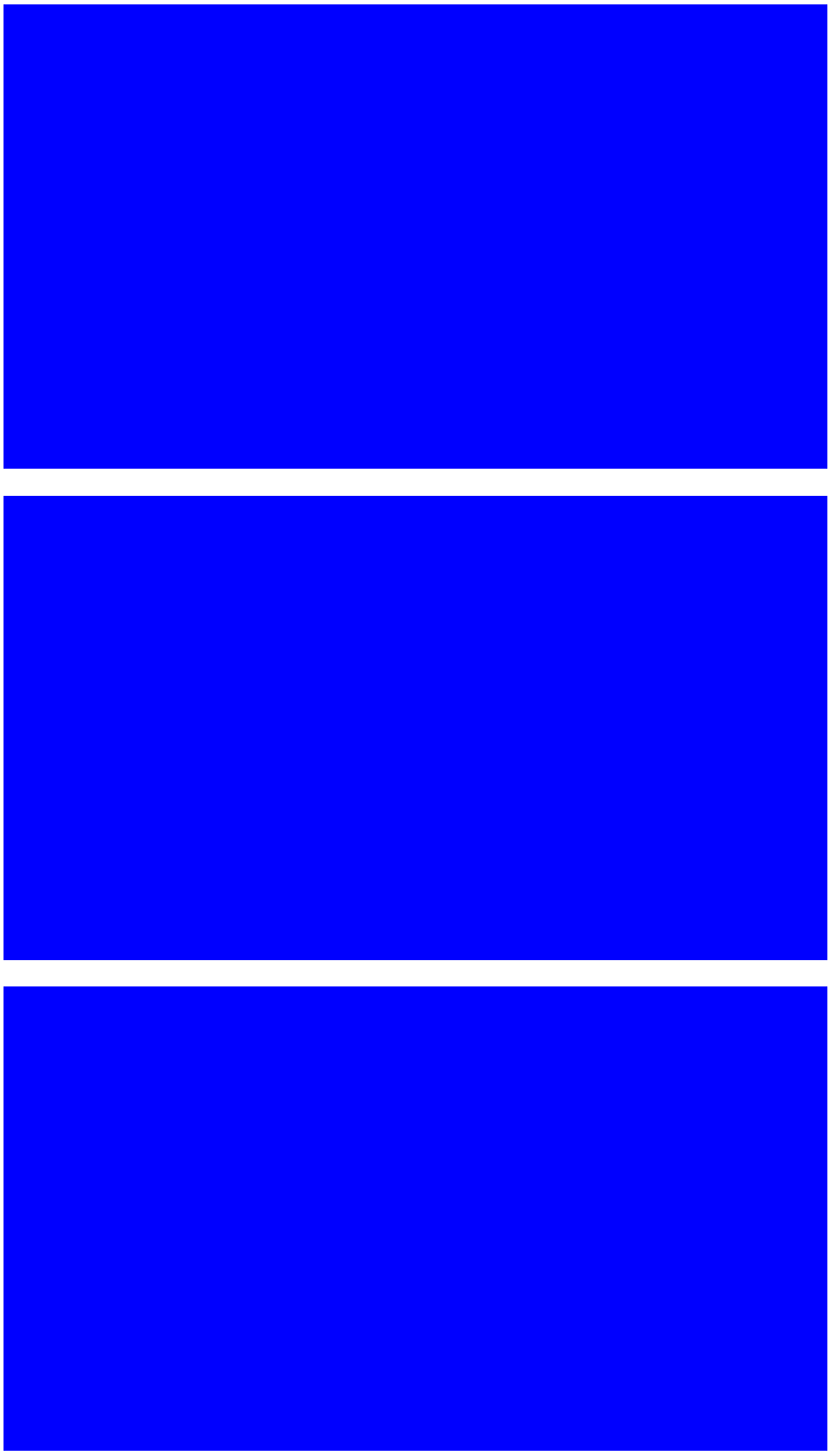

Figure 5.20 – Comparison between the temporal series of temperature recorded at Tavira station and the results of the model for the campaigns performed in May, September and October.

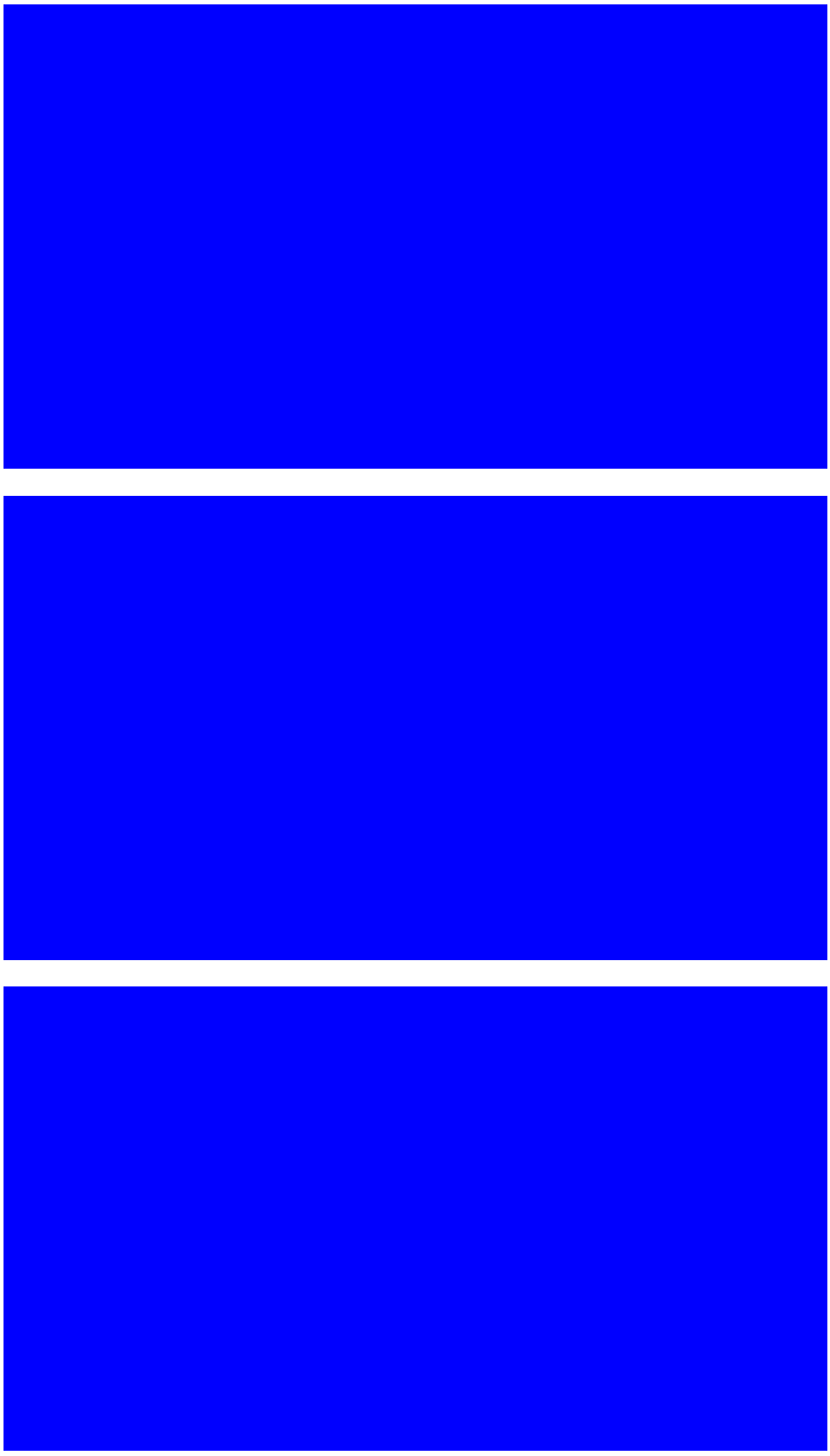

Figure 5.21 – Comparison between the temporal series of temperature recorded at Cacela station and the results of the model for the campaigns performed in May, September and October.

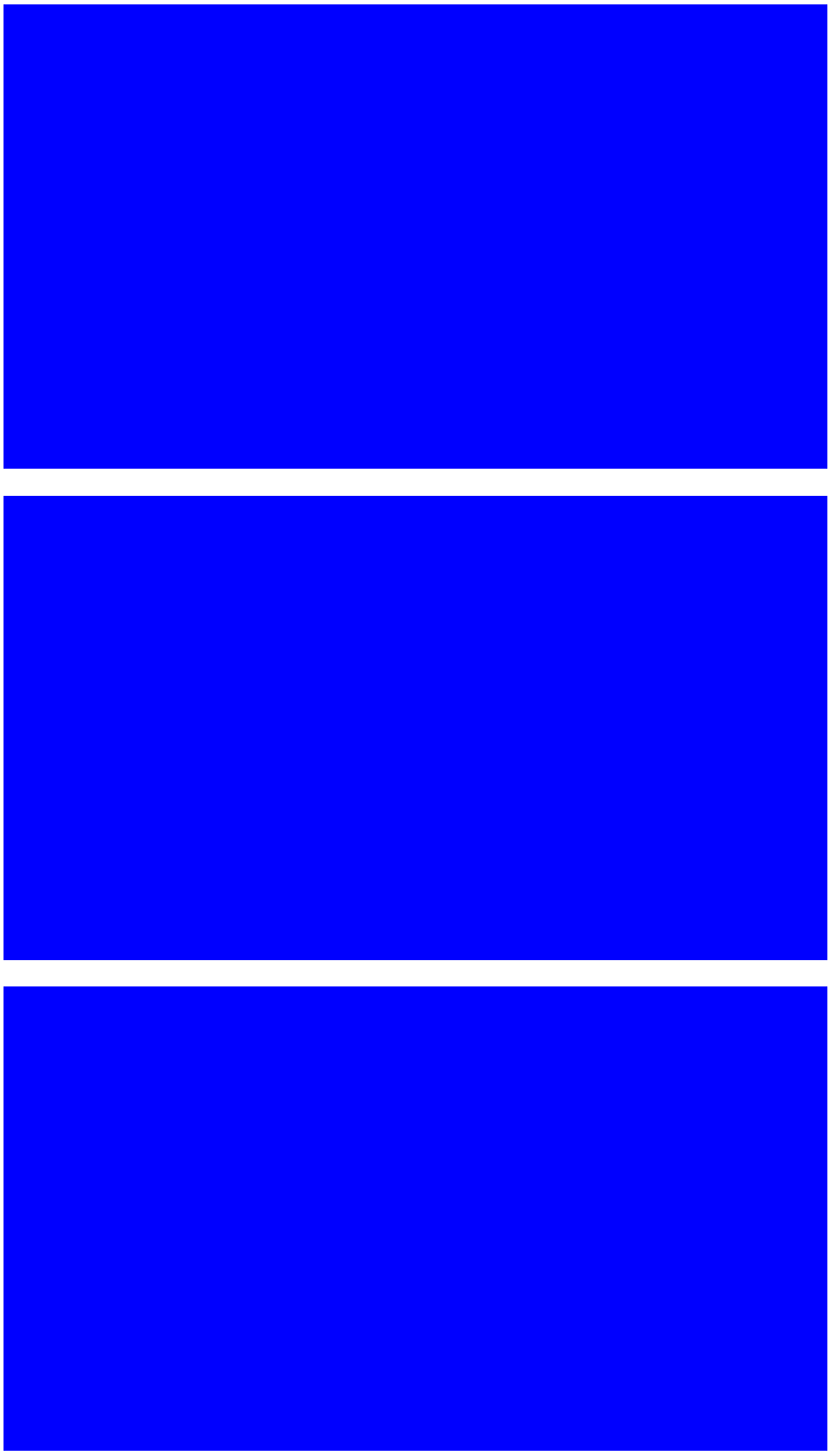

Figure 5.22 – Comparison between the temporal series of temperature recorded at Olhão channel station and the results of the model for the campaigns performed in May, September and October.

6. Conclusions

Within the scope of the project UBEST, the SCHISM 3D model was implemented in the Ria Formosa for the year 2017. This implementation was based on the previous application of Fabio *et al*. (2016) using the SELFE 3D model. Prior to the implementation to the year of 2017, the model was calibrated in barotropic mode by comparison with sea surface elevation data recorded in 1980 and validated using the sea surface elevation and current velocities data recorded in 2011.

To implement the hydrodynamic model for the year of 2017, the grid and bathymetry were updated, and the baroclinic model was validated based on the comparison of the sea surface elevation, temperature and salinity recorded in three seasonal campaigns performed in the scope of project UBEST during 2017 with the time series extracted from the model simulations.

The results show the good performance of the model in representing the hydrodynamic circulation within the lagoon and in the external area. Regarding to the water temperature, the model has some limitations in representing the water heating in the shallow areas of the lagoon and the influence of intense mesoscale events (e.g. upwelling events), which results in an underestimation of the water temperature by the model. The salinity was almost constant in time and space, and evaporation processes must be considered in future applications for a better representation of this variable. Despite these limitations, the baroclinic model can be considered validated in the Ria Formosa coastal lagoon, since the RMSE are within an acceptable range. This hydrodynamic model will be coupled to the biogeochemical model, which will be used to better understand the susceptibility of the biogeochemical buffering capacity of Ria Formosa to future scenarios of climate change and anthropogenic inputs.

Acknowledgments

This work was funded by Fundação para a Ciência e a Tecnologia project UBEST – Understanding the biogeochemical buffering capacity of estuaries relative to climate change and anthropogenic inputs (PTDC/AAG-MAA/6899/2014).

The first author is funded by Fundação para a Ciência e a Tecnologia in the scope of the project UBEST (PTDC/AAG-MAA/6899/2014).

References

Barbosa, A.B., 2010. Seasonal and interannual variability of planktonic microbes in a mesotidal coastal lagoon (Ria Formosa, SE Portugal): impact of climatic changes and local human influences. In: Coastal Lagoons: critical habitats of environmental change, Eds.: H. Paerl and M. Kennish, CRC Press, Taylor & Francis Group, Marine Science Book Series, Boca Raton, 335-366 pp.

Bruneau, A., Fortunato, A.B., Portela L., 2010. Valorização hidrodinâmica da Ria Formosa e mitigação do risco nas ilhas barreira, Relatório 2: Valorização hidrodinâmica da laguna, 1ª e 2ª fases. Relatório 395/2011-NEC, Lisboa.

Chiu, C., Huang, C., Wu, L., Zhang, Y., Chuang, L., Fan, Y., Yu, H-C., 2018. Forecasting of oil-spill trajectories by using SCHISM and X-band radar. *Marine Pollution Bulletin*, 137, 566-581.

Cravo, A., Cardeira, S., Pereira, C., Rosa, M., Alcântara, P., Madureira, M., Jacob, J., 2014. Exchanges of nutrients and chlorophyll a through two inlets of Ria Formosa, South of Portugal, during coastal upwelling events. *Journal of Sea Research*, 93, 63 – 74.

Cravo, A., Jacob, J., Rosa, A., 2017a. Report 3, Field campaign UBEST1: Ria Formosa – May 30-31, 2017. Universidade do Algarve, pp. 11.

Cravo, A., Jacob, J., Rosa, A., 2017b. Report 4, Field campaign UBEST2: Ria Formosa – September 14-15, 2017. Universidade do Algarve, pp. 11.

Cravo, A., Jacob, J., Rosa, A., 2017c. Report 5, Field campaign UBEST3: Ria Formosa – October 25-26, 2017. Universidade do Algarve, pp. 11.

Dee, D. P., Uppala, S. M., Simmons, A. J., Berrisford, P., Poli, P., Kobayashi, S., Andrae, U., Balmaseda, M. A., Balsamo, G., Bauer, P., Bechtold, P., Beljaars, A. C. M., van de Berg, L., Bid lot, J., Bormann, N., Delsol, C., Dragani, R., Fuentes, M., Geer, A. J., Haimberger, L., Healy, S. B., Hersbach, H., Hólm, E. V., Isaksen, L., Kallberg, P., Köhler, M., Matricardi, M., McNally, A. P., Monge-Sanz, B. M., Morcrette, J.-J., Park, B.-K., Peubey, C., de Rosnay, P., Tavolato, C., Thépaut, J.-N., and Vitart, F., 2011. The ERA-Interim reanalysis: configuration and performance of the data assimilation system. *Quarterly Journal of the Royal Meteorological Society*, 137, 553–597.

Dias, J. M., Sousa, M. C., Bertin, X., Fortunato, A. B., Oliveira, A., 2009. Numerical modeling of the impact of the Ancão Inlet relocation (Ria Formosa, Portugal). *Environmental Modelling and Software*, 24(6), 711–725.

Dias, J.M., Lopes, J.F., 2006. Implementation and assessment of hydrodynamic, salt and heat transport models: The case of Ria de Aveiro Lagoon (Portugal). *Environmental Modelling & Software* 21, pp. 1–15.

Fabião, J., Rodrigues, M., Fortunato, A., Jacob, J., Cravo, A., 2016. Water exchanges between a multi-inlet lagoon and the ocean: the role of forcing mechanisms. *Ocean Dynamics*, 66(2), 173–194.

Falcão, M., Vale, C., 1990. Study of the Ria Formosa ecosystem: benthic nutrient remineralization and tidal variability of nutrients in the water. *Hydrobiologia*, 207(1), 137–146.

Ferreira, J. G., Simas, T., Nobre, A., Silva, M. C., Shifferegger, K., Lencart-Silva, J., 2003. Identification of sensitive areas and vulnerable zones in transitional and coastal Portuguese systems. Application of the United States National Estuarine Eutrophication Assessment to the Minho, Lima, Douro, Ria de Aveiro, Mondego, Tagus, Sado, Mira, Ria Formosa and Guadiana systems. INAG and IMAR, 79–94.

Ferreira, J.G., Abreu, P.F., Bettencourt, A.M., Bricker, S.B., Marques, J.C., Melo, J.J., Newton, A., Nobre, A., Patricio, J., Rocha, F., Rodrigues, R., Sais, F., Silva, M.C., Simas, T., Soares, C.V., Stacey, P.E., Vale, C., de Wit, M., Wolff, W.J., 2005. Monitoring plan for water quality and ecology of Portuguese transitional and coastal waters (MONAE), 164 pp.

Ferreira, J.G., Nobre, A.M., Simas, T.C., Silva, M.C., Newton, A., Bricker, S.B., Wolff, W.J., Stacey, P.E., Sequeira, A., 2006. A methodology for defining homogeneous water bodies in estuaries - Application to the transitional systems of the EU Water Framework Directive. *Estuarine, Coastal and Shelf Science*, 66(3-4), 468-482.

Fortunato, A. B., Li, K., Bertin, X., Rodrigues, M., Miguez, B. M., 2016. Determination of extreme sea levels along the Iberian Atlantic coast. *Ocean Eng*. 111, 471–482.

Fortunato, A.B., Pinto, L., Oliveira, A., Ferreira, J.S., 2002. Tidally generated shelf waves off the western Iberian coast. *Continental Shelf Research* 22, pp.1935–1950.

Jacob, J. and Cravo, A., 2019. Recent evolution of the tidal prisms at the inlets of the western sector of the Ria Formosa, south coast of Portugal. *Regional Studies in Marine Science* 31, 100767.

Jacob, J., Cardeira, S., Rodrigues, M., Bruneau, N., Azevedo, A., Fortunato, A., 2012. Contribuição para o estudo da propagação da maré no setor oeste da Ria Formosa. 2as Jornadas de Engenharia Hidrográfica, (1), 185–188.

Jacob, J., Cardeira, S., Rodrigues, M., Bruneau, N., Azevedo, A., André, B. F., Cravo, A., 2013. Experimental and numerical study of the hydrodynamics of the western sector of Ria Formosa. *Journal of Coastal Research*, Special Issue, (65), 2011–2016.

Li, J., Yang, W., Li, W., Mu, L., and Jin, Z., 2018. Coupled hydrodynamic and water quality simulation of algal bloom in the Three Gorges Reservoir, China. *Ecological Engineering*, 119, 97-108.

Linares, A., Wu, C.H., Bechle, A.J., Anderson, E.J., Kristovich, D.A., 2019. Unexpected rip currents induced by a meteotsunami. *Nature- Scientific Reports* 9, p. 2105.

Malta, E. jan, Stigter, T. Y., Pacheco, A., Dill, A. C., Tavares, D., Santos, R., 2017. Effects of External Nutrient Sources and Extreme Weather Events on the Nutrient Budget of a Southern European Coastal Lagoon. *Estuaries and Coasts*, 1 – 18.

Martins, F., Pina, P., Calado, S., Delgado, S., Neves, R., 2003. A coupled hydrodynamic and ecological model to manage water quality in Ria Formosa coastal lagoon. *Advances in Ecological Sciences*, 18, 93-100.

Mudge, S.M., Icely, J.D., Newton, A., 2008. Residence times in a hypersaline lagoon: Using salinity as a tracer. *Estuarine, Coastal and Shelf Science*, 77(2), 278–284.

Newton, A., Icely, J., Cristina, S., Brito, A., Cardoso, A. C., Colijn, F., Zaldívar, J. M., 2014. An overview of ecological status, vulnerability and future perspectives of European large shallow, semi-enclosed coastal systems, lagoons and transitional waters. *Estuarine, Coastal and Shelf Science*, 140, 95–122.

Newton, A., Mudge, S. M., 2003. Temperature and salinity regimes in a shallow, mesotidal lagoon, the Ria Formosa, Portugal. *Estuarine, Coastal and Shelf Science*, 57(1–2), 73–85.

Pacheco, A., Ferreira, Ó., Williams, J. J., Garel, E., Vila-Concejo, A., Dias, J. A., 2010. Hydrodynamics and equilibrium of a multiple-inlet system. *Marine Geology*, 274(1–4), 32–42.

Rodrigues, M., Fortunato, A.B., 2017. Assessment of a three-dimensional baroclinic circulation model of the Tagus estuary (Portugal). *AIMS Environmental Science* 4, (6), pp. 763 - 787.

Rodrigues, M., Oliveira, A., Queiroga, H., Brotas, V., 2012. Seasonal and diurnal water quality modelling along a salinity gradient (Mira channel, Aveiro lagoon, Portugal. *Procedia Environmental Sciences*, 899-918.

Rodrigues, M., Oliveira, A., Queiroga, H., Fortunato, A.B., Zhang, Y.J., 2009. Three-dimensional modeling of the lower trophic levels in the Ria de Aveiro (Portugal). *Ecological Modelling*, 220, pp. 1274-1290.

Salles, P., 2001. Hydrodynamic Controls On Multiple Tidal Inlet Persistence. Massachusetts Institute of Technology and Woods Hole Oceanographic Institution, PhD thesis, 272p.

Salles, P., Voulgaris, G., Aubrey, D. G., 2005. Contribution of nonlinear mechanisms in the persistence of multiple tidal inlet systems. *Estuarine, Coastal and Shelf Science*, 65(3), 475–491.

Silva, M., Patrício, P., Mariano, A.C., Valério, M., Morais, M., 2012. Obtenção de Dados LIDAR para as Zonas Costeiras de Portugal Continental, 2.as Jornadas de Engenharia Hidrográfica, Lisboa, 2012, pp. 19-22.

Tett, P., Gilpin, L., Svendsen, H., Erlandsson, C. P., Larsson, U., Kratzer, S., Scory, S., 2003. Eutrophication and some European waters of restricted exchange. *Continental Shelf Research*, 23 (17–19), 1635–1671.

Vila-concejo, A., Matias, A., Ferreira, Ó., Duarte, C., Dias, J.M.A., 2002. Recent evolution of the natural inlets of a barrier island system in Southern Portugal. *Journal of Coastal Research*, SI 36, pp. 741-752.

Zhang, Y. and Baptista, A.M., 2008. SELFE: A semi-implicit Eulerian-Lagrangian finite-element model for cross-scale ocean circulation". *Ocean Modelling*, 21(3-4), 71-96.

Zhang, Y., Ateljevich, E., Yu, H-C., Wu, C-H., Yu, J.C.S., 2015. A new vertical coordinate system for a 3D unstructured-grid model. *Ocean Modelling*, 85, 16-31.

Zhang, Y., Ye, F., Stanev, E.V., Grashorn, S., 2016. Seamless cross-scale modeling with SCHISM. *Ocean Modelling*, 102, 64-81.

ANNEX I – Additional results of salinity

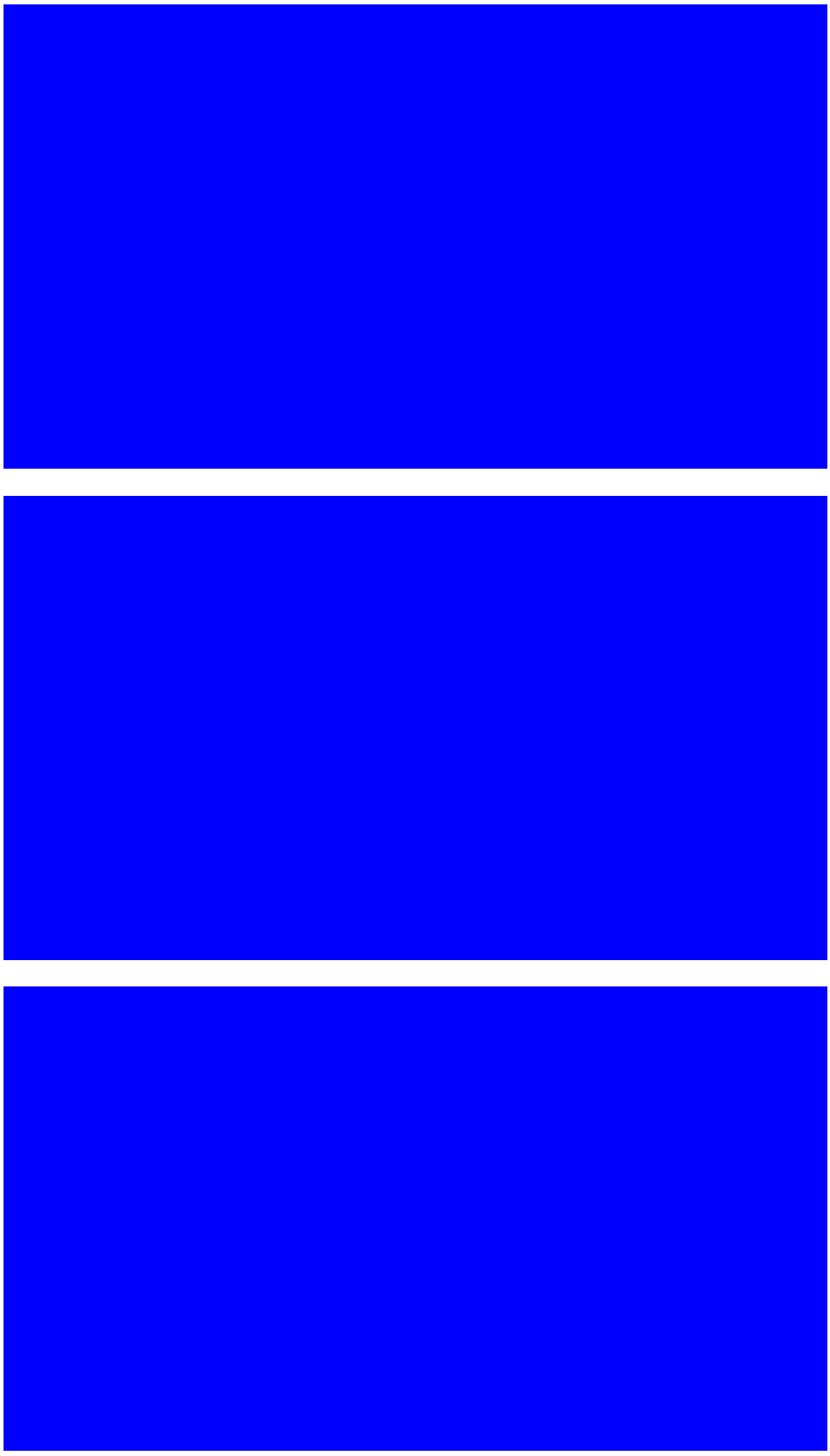

Figure A.I. 1 – Comparison between the temporal series of salinity recorded at Boundary station and the model results for different oceanic boundary conditions (data measured at BS during the field campaigns (FD); data measured by the Deserta Island PT (PT); constant values (IBI-C) and time and space varying values (IBI-V) from IBI-MFC) for the campaigns performed in May, September and October.

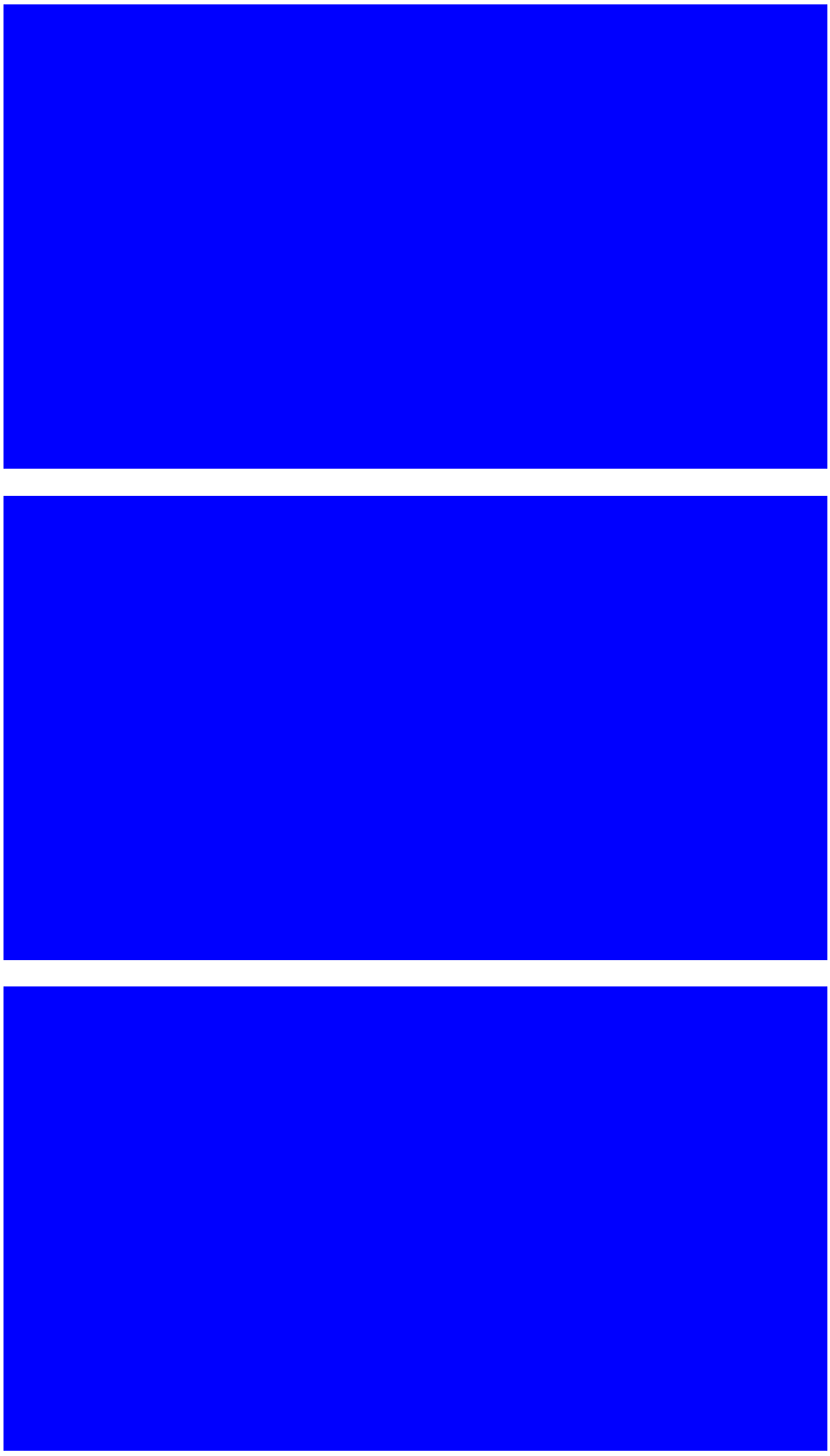

Figure A.I. 2 – Comparison between the temporal series of salinity recorded at Faro Beach station and the model results for different oceanic boundary conditions (data measured at BS during the field campaigns (FD); data measured by the Deserta Island PT (PT); constant values (IBI-C) and time and space varying values (IBI-V) from IBI-MFC) for the campaigns performed in May, September and October.

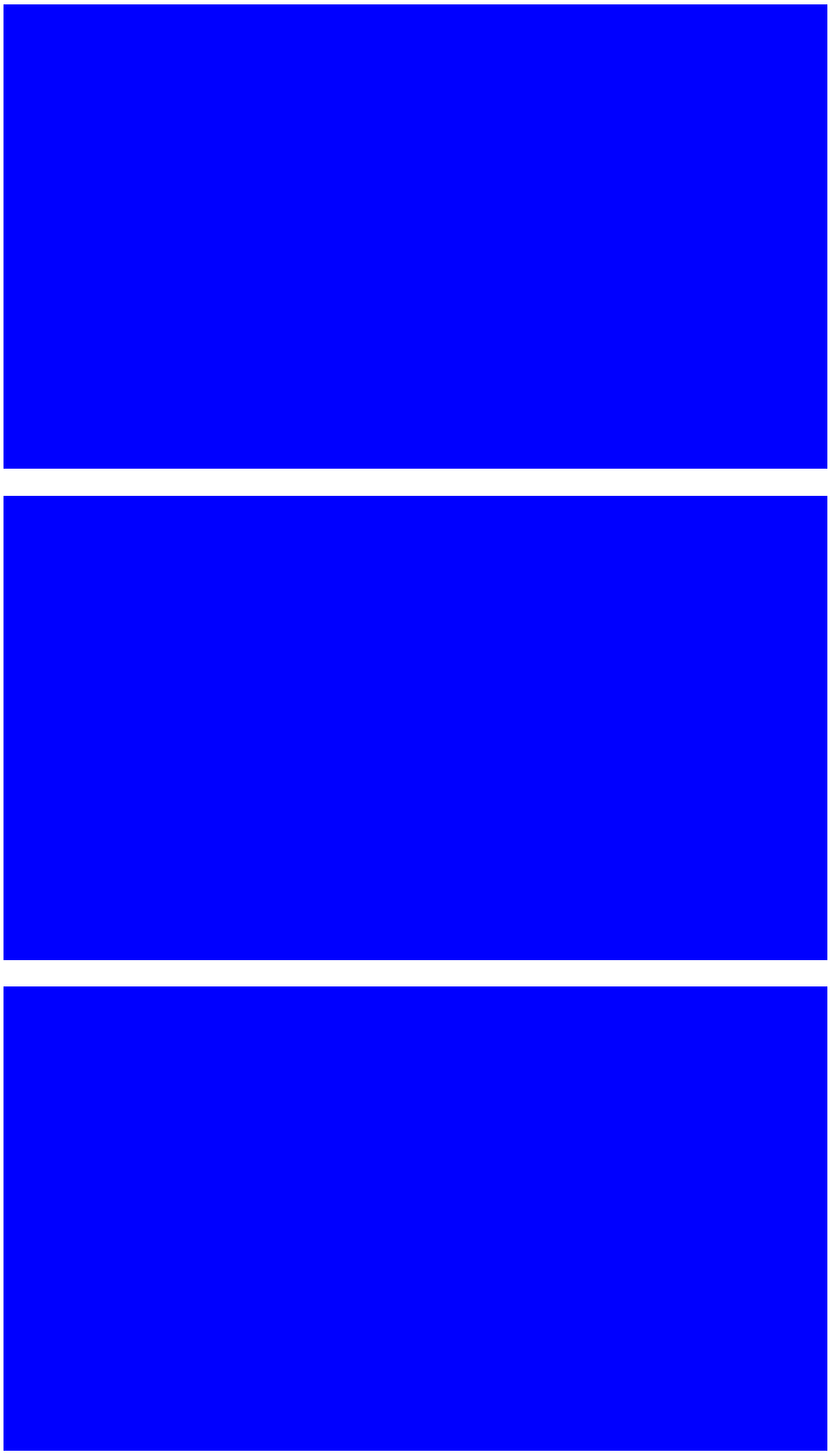

Figure A.I. 3 – Comparison between the temporal series of salinity recorded at Faro Commercial Port station and the model results for different oceanic boundary conditions (data measured at BS during the field campaigns (FD); data measured by the Deserta Island PT (PT); constant values (IBI-C) and time and space varying values (IBI-V) from IBI-MFC) for the campaigns performed in May, September and October.

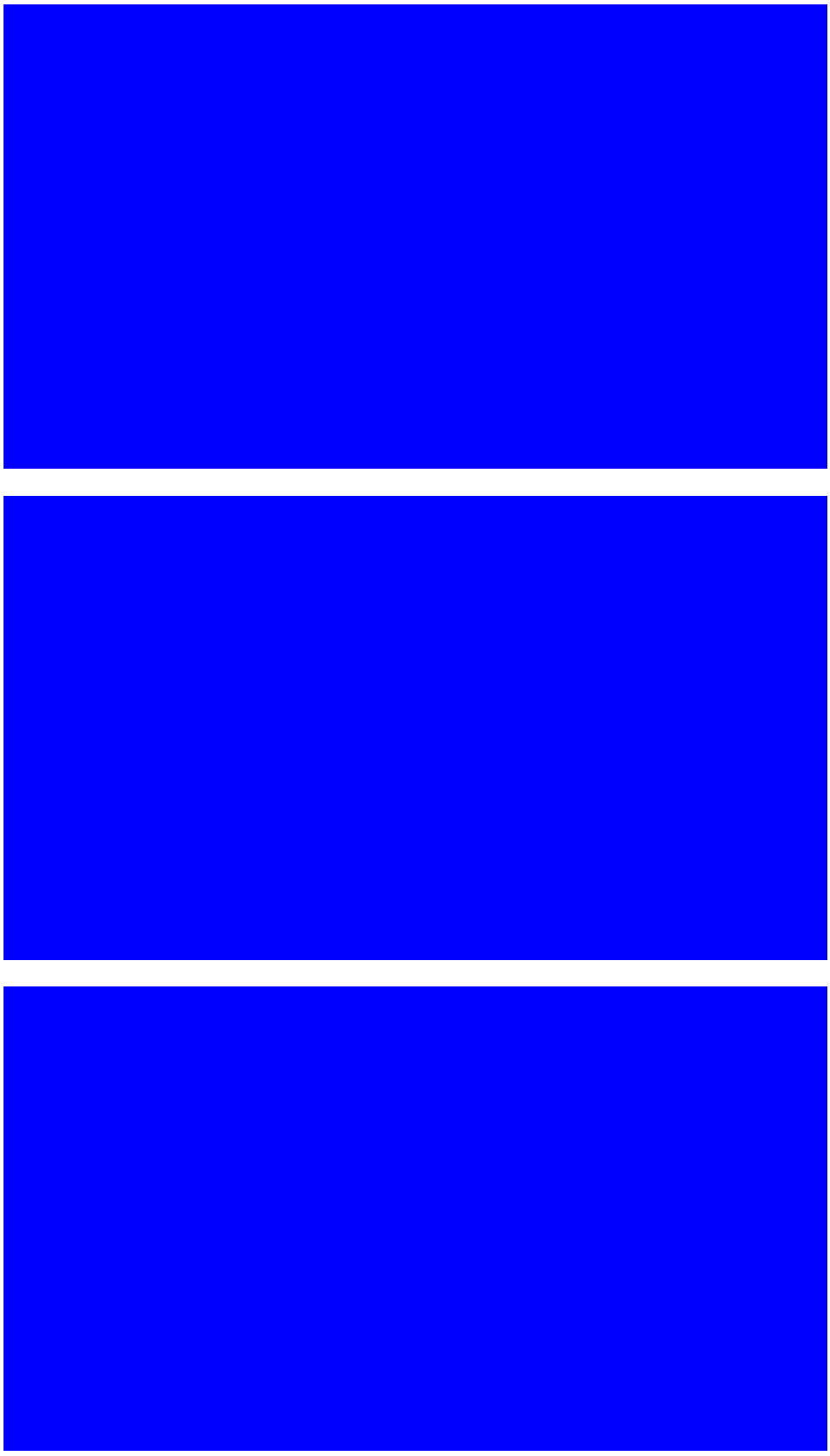

Figure A.I. 4 – Comparison between the temporal series of salinity recorded at Fuzeta station and the model results for different oceanic boundary conditions (data measured at BS during the field campaigns (FD); data measured by the Deserta Island PT (PT); constant values (IBI-C) and time and space varying values (IBI-V) from IBI-MFC) for the campaigns performed in May, September and October.

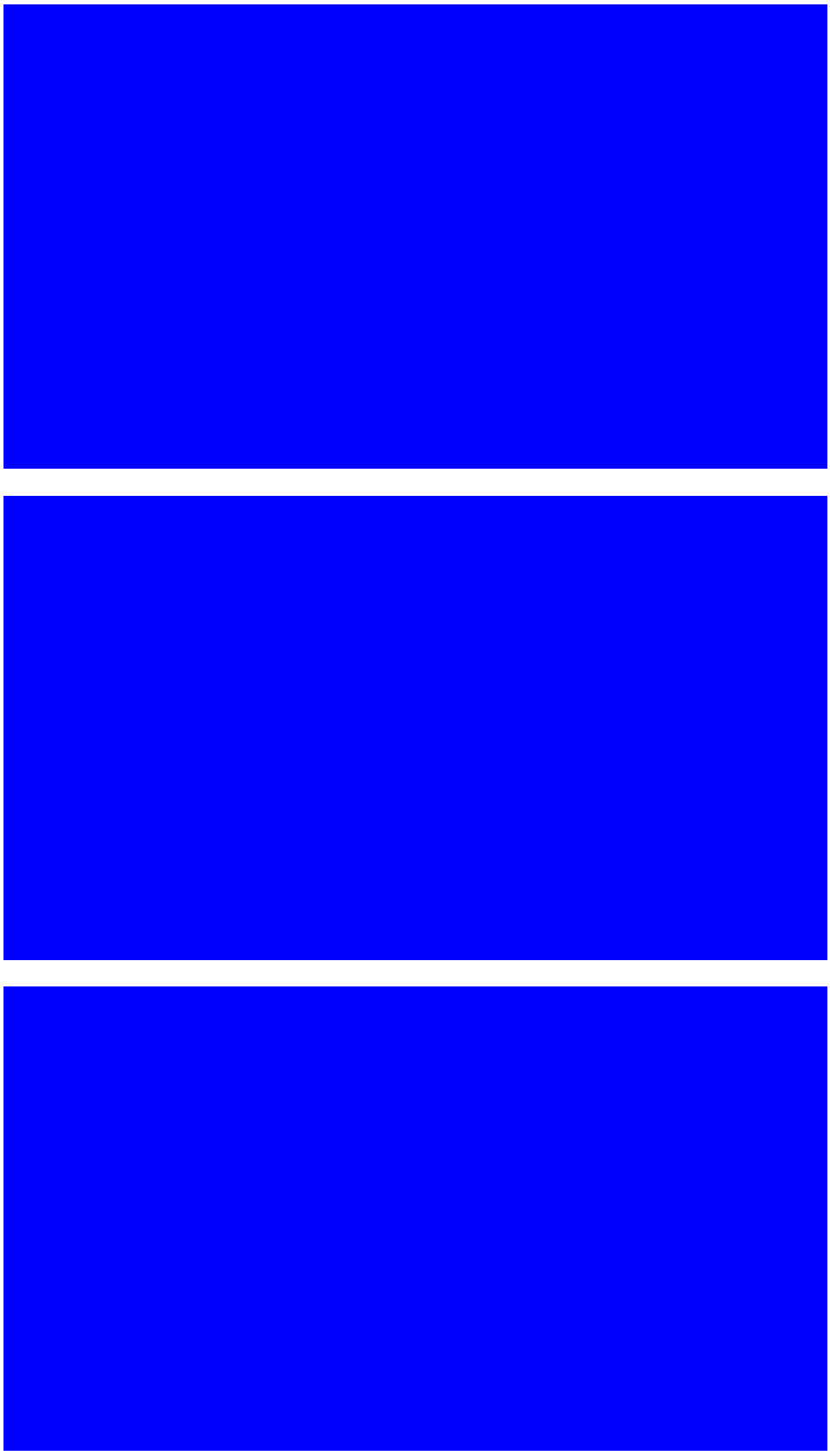

Figure A.I. 5 – Comparison between the temporal series of salinity recorded at Tavira station and the model results for different oceanic boundary conditions (data measured at BS during the field campaigns (FD); data measured by the Deserta Island PT (PT); constant values (IBI-C) and time and space varying values (IBI-V) from IBI-MFC) for the campaigns performed in May, September and October.

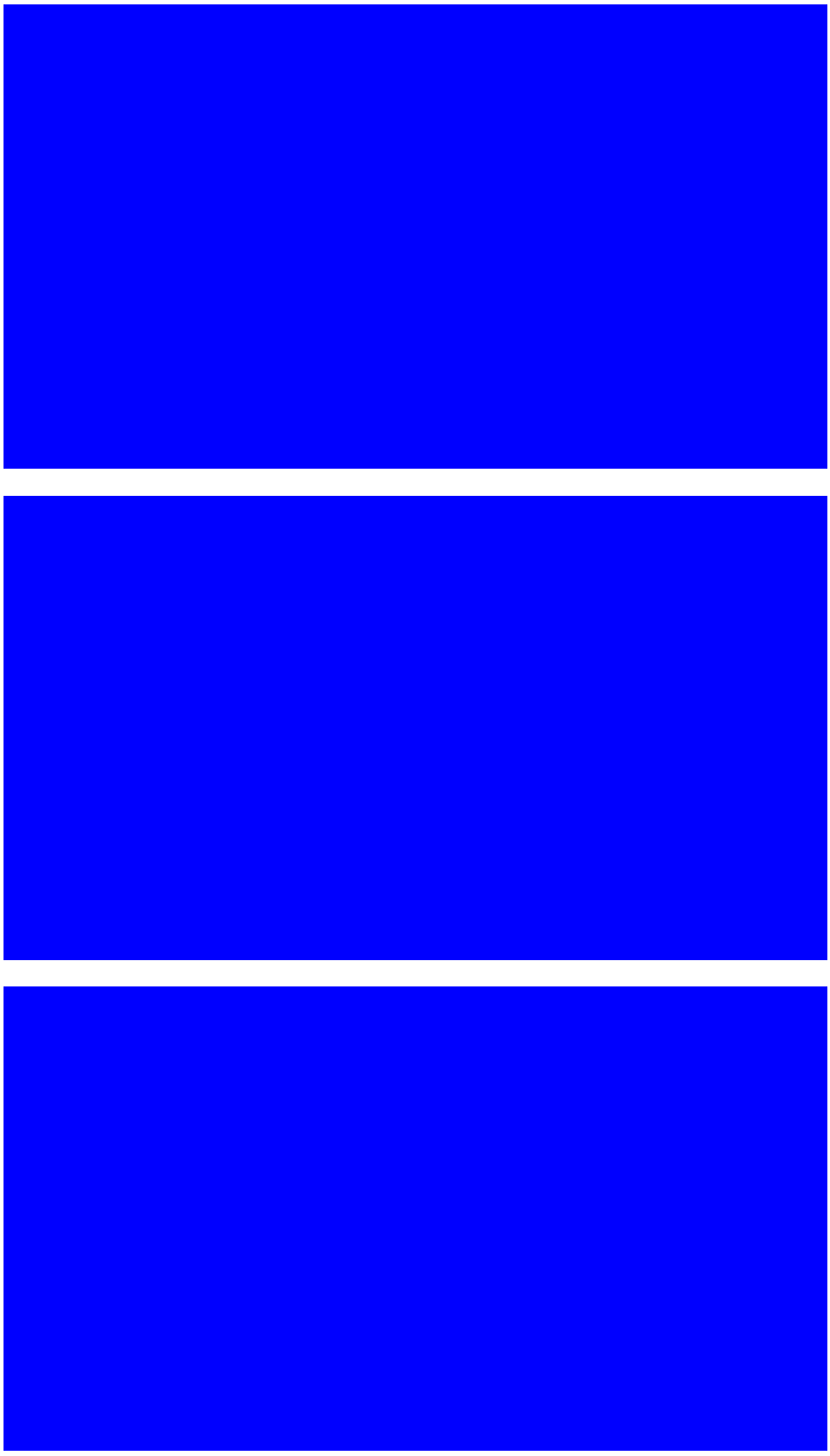

Figure A.I. 6 – Comparison between the temporal series of salinity recorded at Cacela station and the model results for different oceanic boundary conditions (data measured at BS during the field campaigns (FD); data measured by the Deserta Island PT (PT); constant values (IBI-C) and time and space varying values (IBI-V) from IBI-MFC) for the campaigns performed in May, September and October.

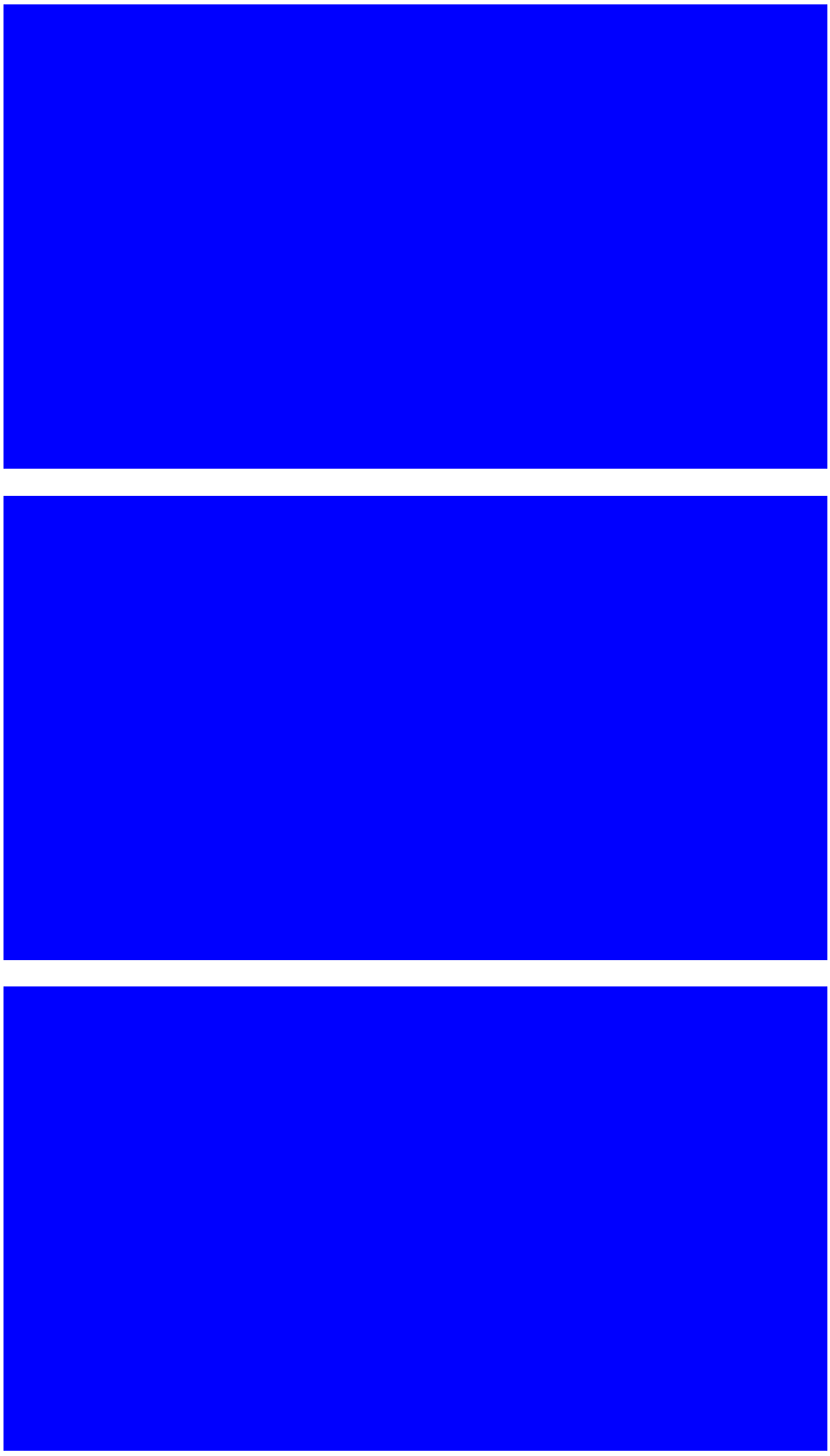

Figure A.I. 7 – Comparison between the temporal series of salinity recorded at Olhão Channel station and the model results for different oceanic boundary conditions (data measured at BS during the field campaigns (FD); data measured by the Deserta Island PT (PT); constant values (IBI-C) and time and space varying values (IBI-V) from IBI-MFC) for the campaigns performed in May, September and October.

ANNEX II – Additional results of water temperature

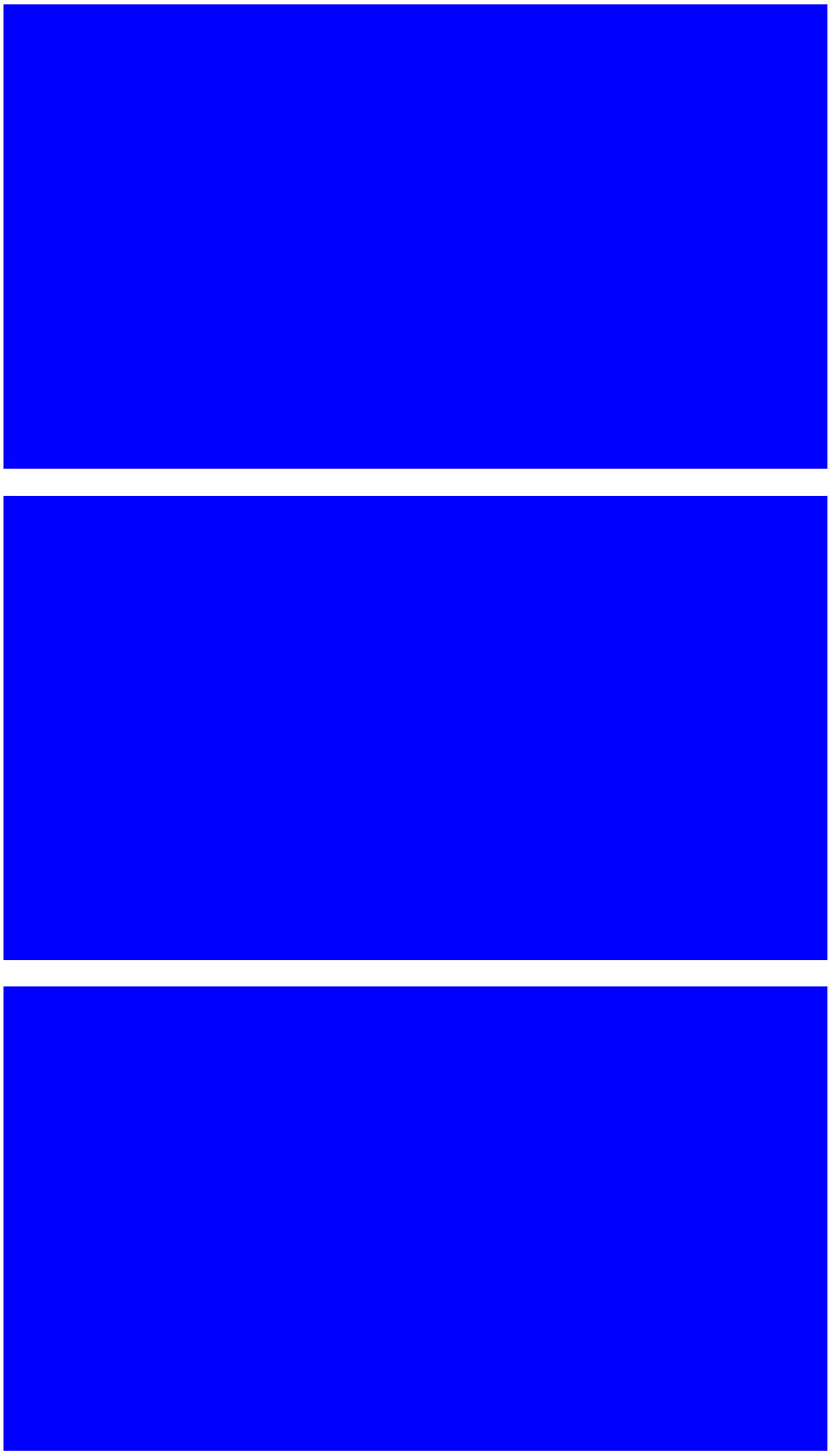

Figure A.II. 1 – Comparison between the temporal series of temperature recorded at Boundary station and the model results for different oceanic boundary conditions (data measured at BS during the field campaigns (FD); data measured by the Deserta Island PT (PT); constant values (IBI-C) and time and space varying values (IBI-V) from IBI-MFC) for the campaigns performed in May, September and October.

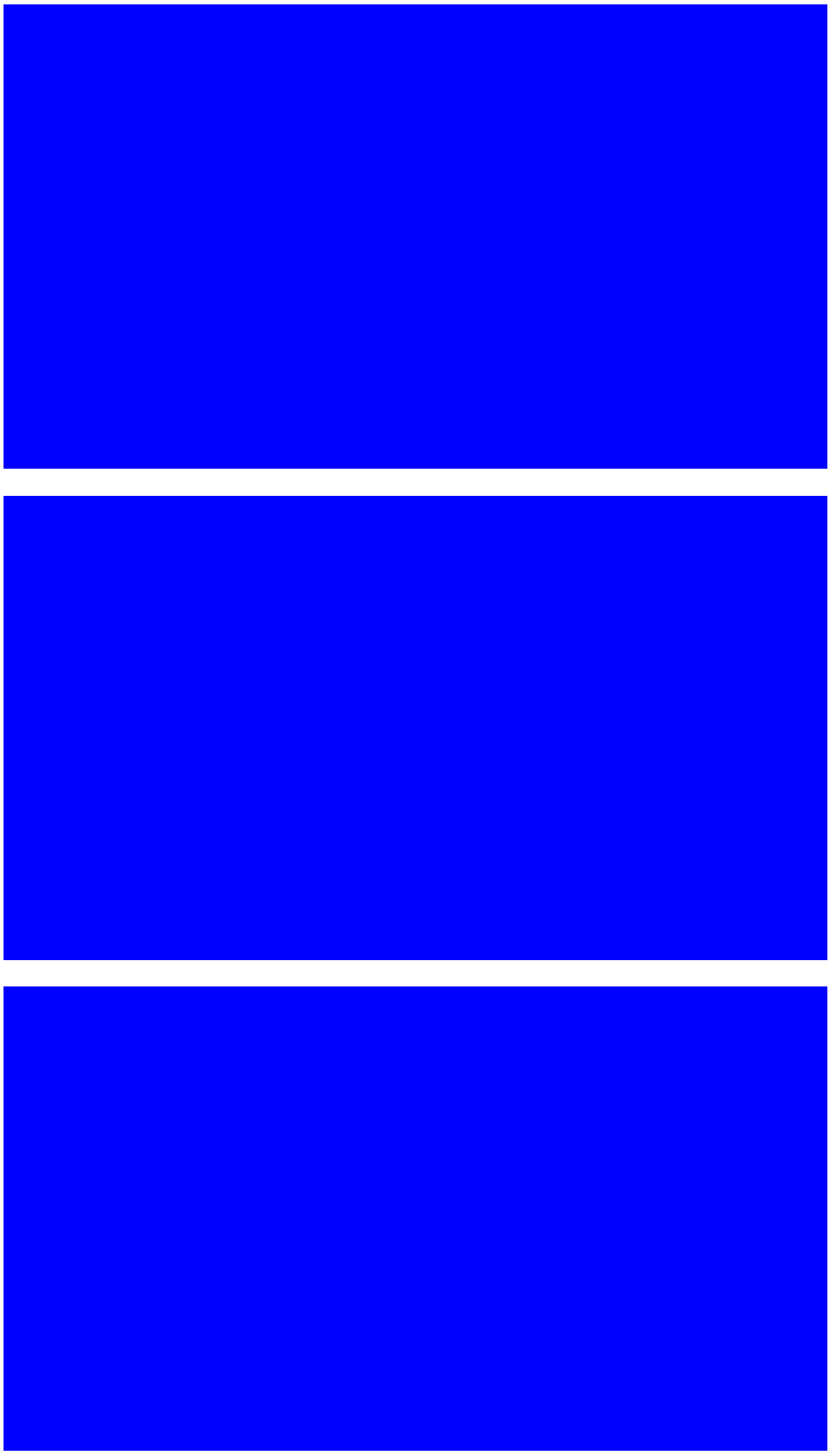

Figure A.II. 2 – Comparison between the temporal series of temperature recorded at Faro Beach station and the model results for different oceanic boundary conditions (data measured at BS during the field campaigns (FD); data measured by the Deserta Island PT (PT); constant values (IBI-C) and time and space varying values (IBI-V) from IBI-MFC) for the campaigns performed in May, September and October.

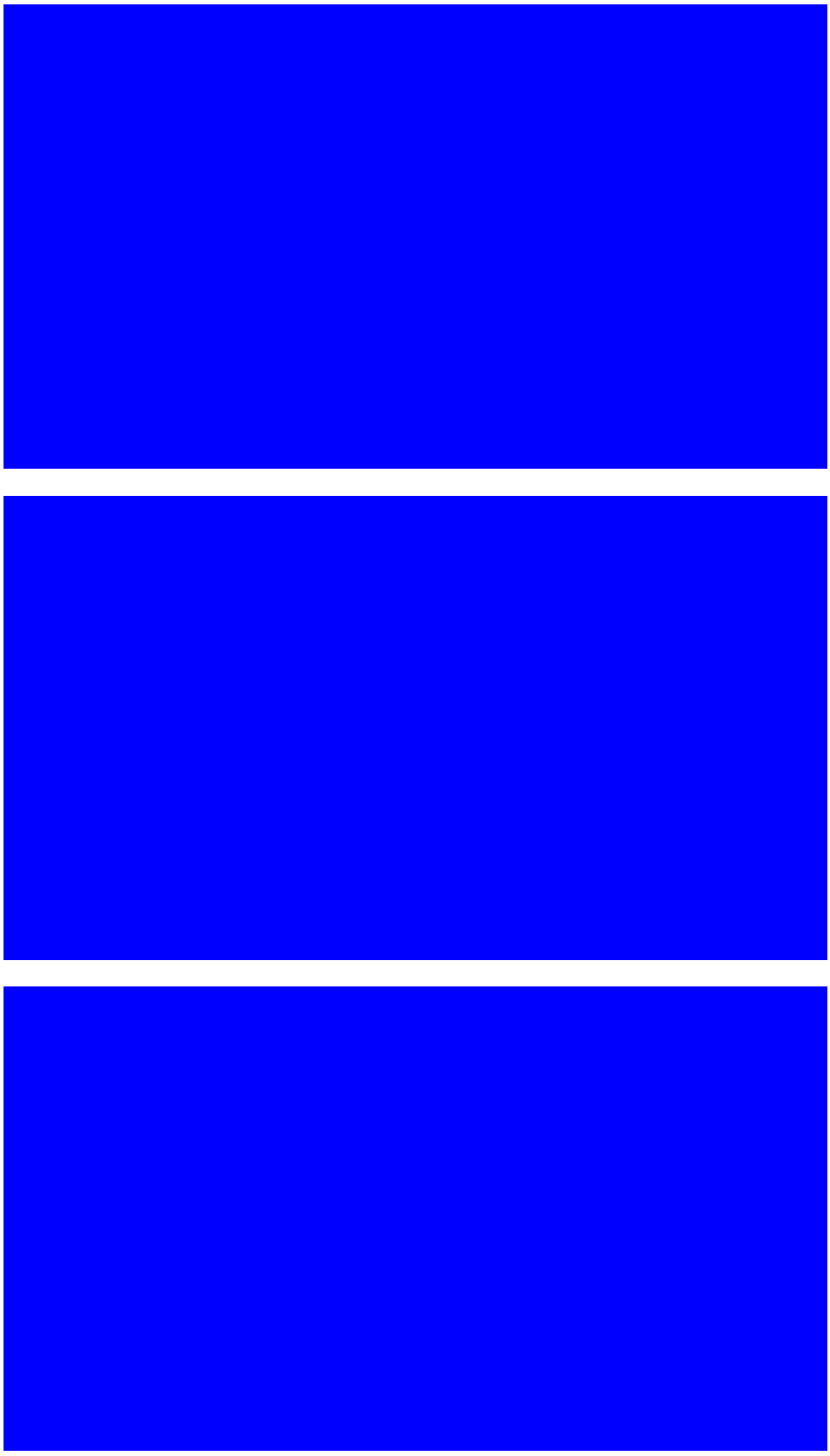

Figure A.II. 3 – Comparison between the temporal series of temperature recorded at Faro Commercial Port station and the model results for different oceanic boundary conditions (data measured at BS during the field campaigns (FD); data measured by the Deserta Island PT (PT); constant values (IBI-C) and time and space varying values (IBI-V) from IBI-MFC) for the campaigns performed in May, September and October.

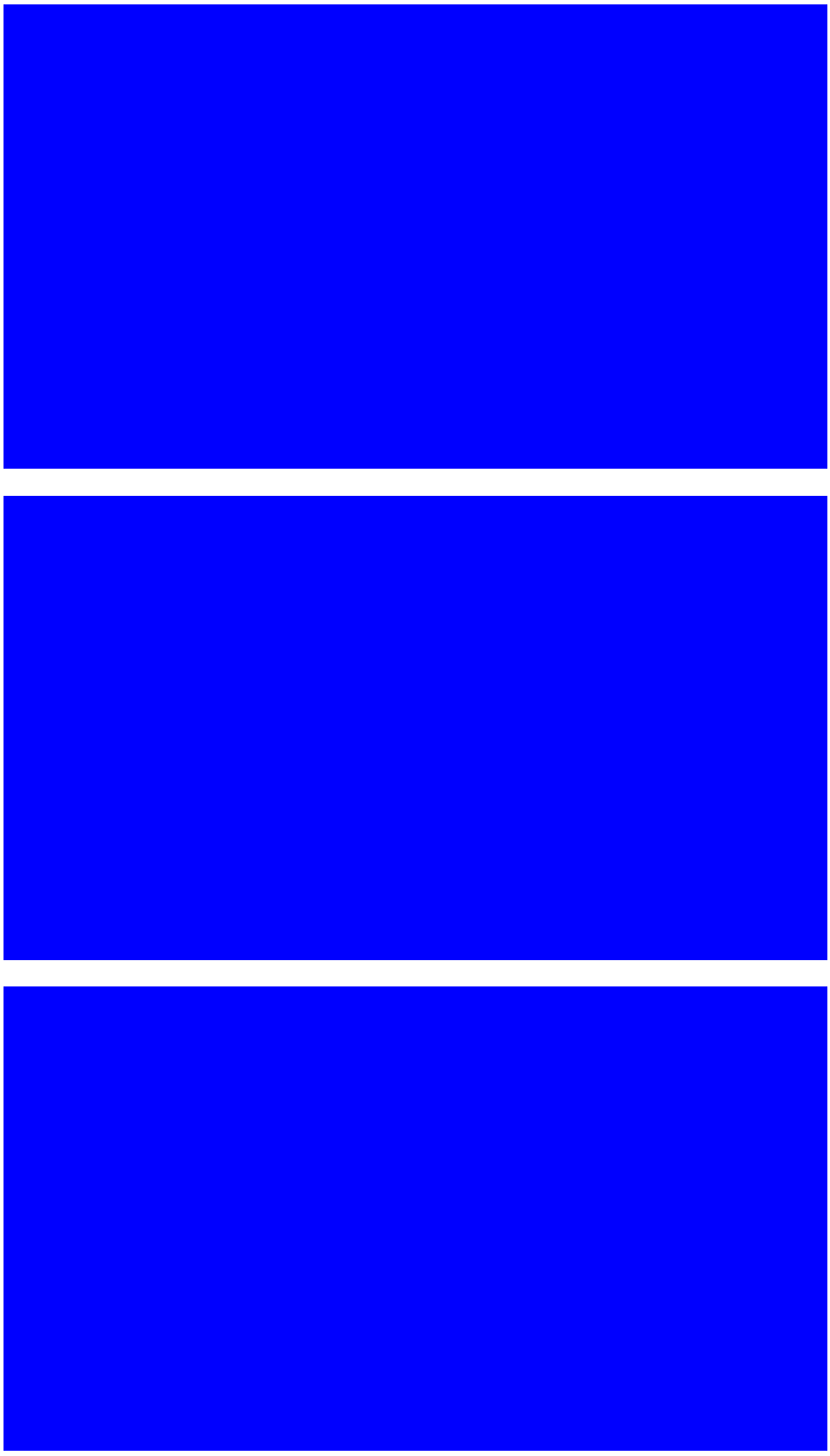

Figure A.II. 4 – Comparison between the temporal series of temperature recorded at Real-Time Observatory station and the model results for different oceanic boundary conditions (data measured at BS during the field campaigns (FD); data measured by the Deserta Island PT (PT); constant values (IBI-C) and time and space varying values (IBI-V) from IBI-MFC) for the campaigns performed in May, September and October.

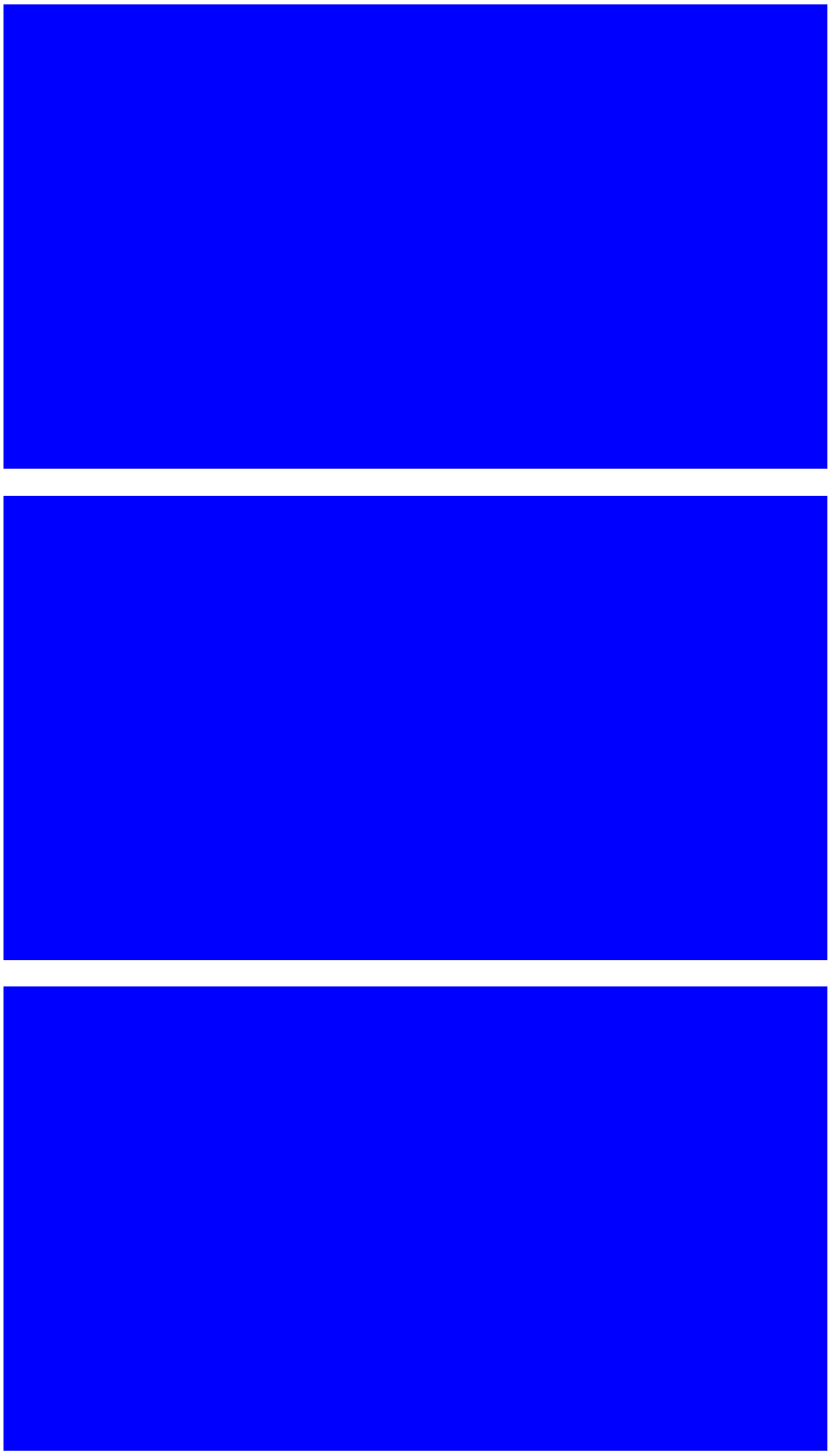

Figure A.II. 5 – Comparison between the temporal series of temperature recorded at Fuzeta station and the model results for different oceanic boundary conditions (data measured at BS during the field campaigns (FD); data measured by the Deserta Island PT (PT); constant values (IBI-C) and time and space varying values (IBI-V) from IBI-MFC) for the campaigns performed in May, September and October.

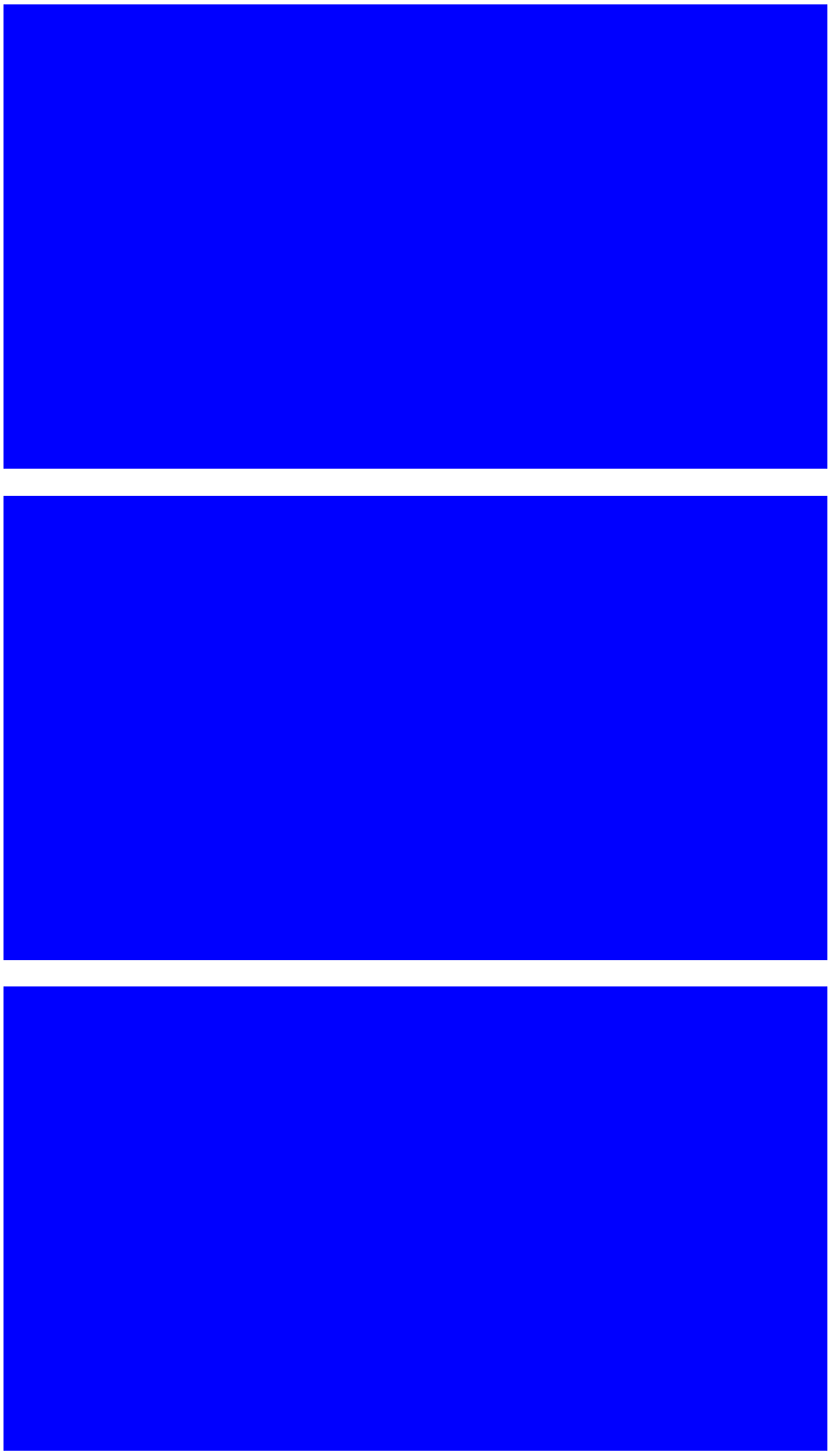

Figure A.II. 6 – Comparison between the temporal series of temperature recorded at Tavira station and the model results for different oceanic boundary conditions (data measured at BS during the field campaigns (FD); data measured by the Deserta Island PT (PT); constant values (IBI-C) and time and space varying values (IBI-V) from IBI-MFC) for the campaigns performed in May, September and October.

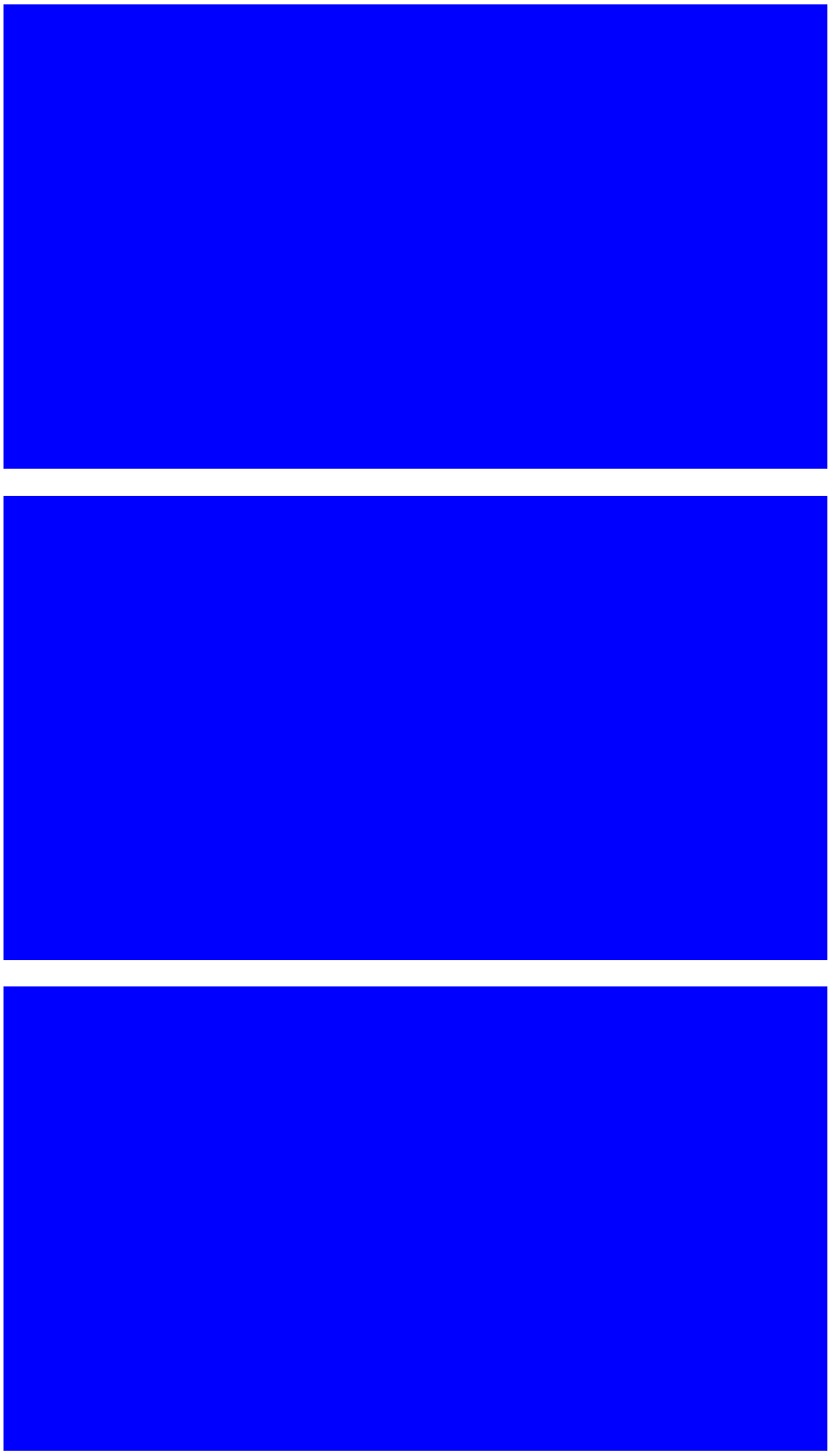

Figure A.II. 7 – Comparison between the temporal series of temperature recorded at Cacela station and the model results for different oceanic boundary conditions (data measured at BS during the field campaigns (FD); data measured by the Deserta Island PT (PT); constant values (IBI-C) and time and space varying values (IBI-V) from IBI-MFC) for the campaigns performed in May, September and October.

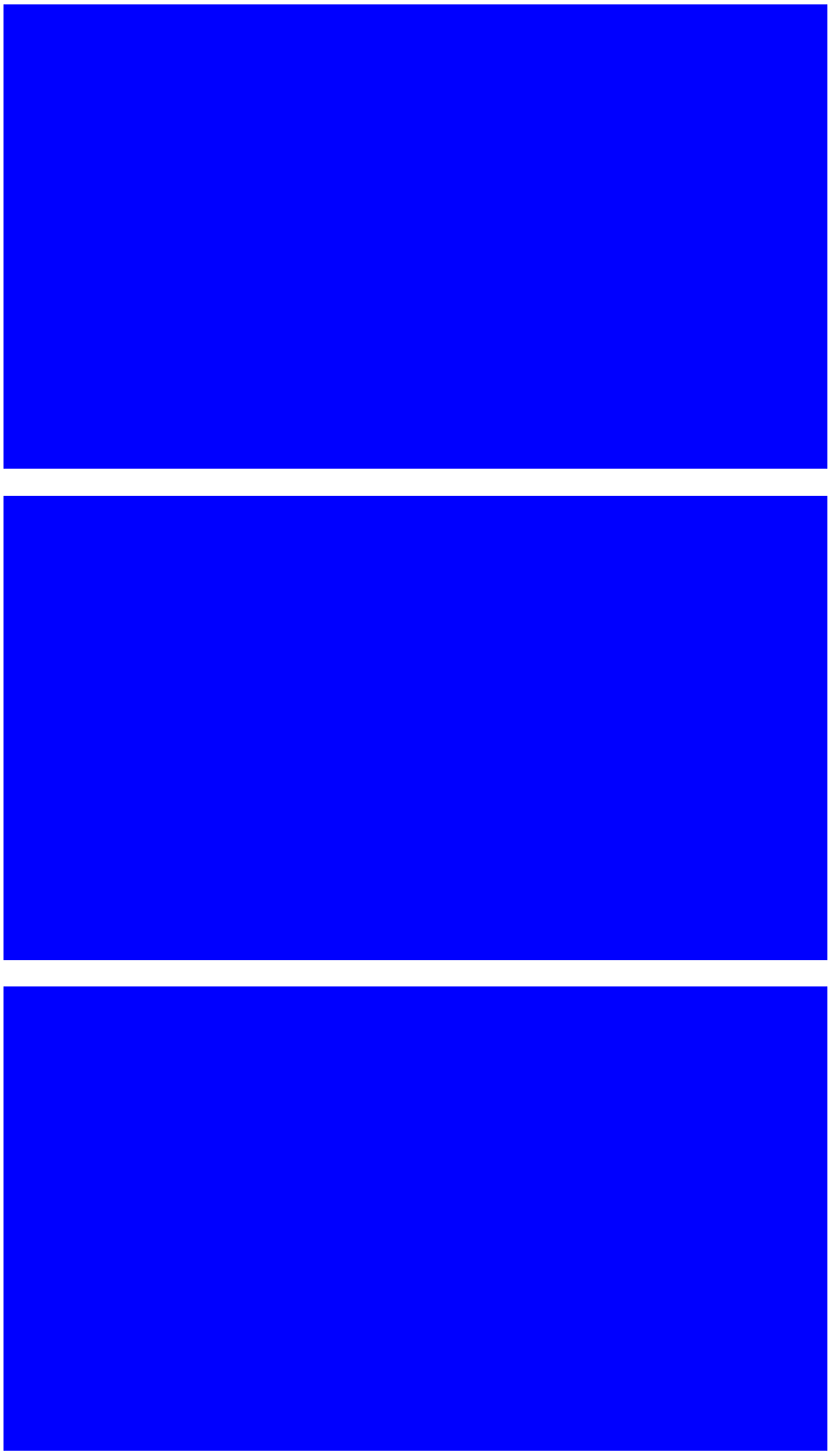

Figure A.II. 8 – Comparison between the temporal series of temperature recorded at Olhão Channel station and the model results for different oceanic boundary conditions (data measured at BS during the field campaigns (FD); data measured by the Deserta Island PT (PT); constant values (IBI-C) and time and space varying values (IBI-V) from IBI-MFC) for the campaigns performed in May, September and October.